

Reprinted from:

Plates and shells with cracks

NOORDHOFF INTERNATIONAL PUBLISHING
LEYDEN

4 *Asymptotic approximations to crack problems in shells*

4.1 Introduction

In nature, shells are the rule rather than the exception. The list of natural shell-like structures is long, and the strength properties of some of them are remarkable. It is logical, therefore, for man to utilize them in man-made structures. But to do this safely, we must understand the fundamental laws which govern the strength and displacement behavior of such structures for they are not immune to failures, particularly in the fracture mode.

It is the intent, therefore, of this chapter to discuss a theoretical method which enables one to determine the stress field that exists in the neighborhood of a crack and furthermore catalog the stress intensity factors for various shell configurations and loads.

In section 2, the author gives a concise summary of the classical shell theory and its limitations. He then goes on to discuss the general character of the equations and subsequently shows that for the two simple geometries, spherical and cylindrical, the equations reduce considerably and in the limit the governing equations of a flat plate are recovered.

Because the solution for a general arbitrary initial curvature presents formidable mathematical complexities, in section 3 he chooses to display the analytical method by specializing it to a spherical shell. In order to preserve unity, he does this in some great length giving sufficient details.

In sections 5 and 6 he gives the stress intensity factors for a cylindrical shell with various crack orientations and for other more complicated shell geometries.

In section 7, he examines what effect, if any, elastic foundations have on the stress intensity factors. Such information can be of great practical value to highway construction and the designing of storage tanks for the oil industry.

4.2 General theory—classical

In the following, we consider bending and stretching of thin shells of revolution, as described by the traditional two-dimensional linear theory and with the additional assumption of shallowness*. In speaking of the formulation of two-dimensional differential equations, we mean the transition from the exact three-dimensional elasticity problem to that of two-dimensional approximate formulation, which is appropriate in view of the ‘thinness’ of the shell. We shall, furthermore, limit our considerations to homogeneous, isotropic, constant thickness, shallow segments of shells, subjected to small deformations and strains so that the stress-strain relations may be established through Hooke’s law.

The basic variables in the theory of shallow shells are the displacement function $w(X, Y)$ in the direction of an axis Z and a stress function $F(X, Y)$ which represents the stress resultants tangent to the middle surface of the shell. Following Marguerre [2], the coupled differential equations governing w and F , with X and Y as rectangular cartesian coordinates of the base plane (see Figure 4.1), are given by:

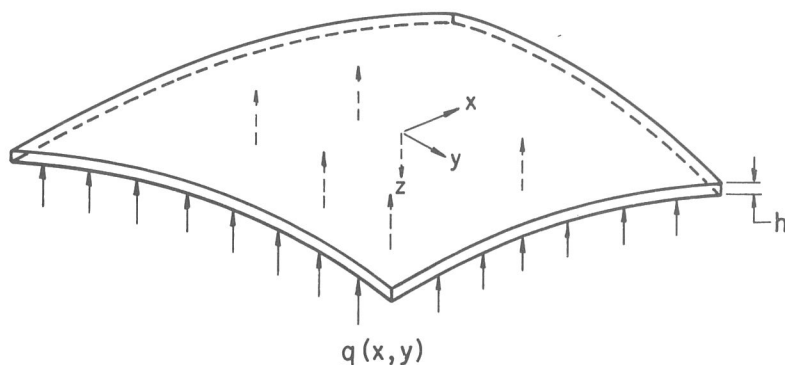


Figure 4.1. Initially Curved Sheet

$$\nabla^4 F = Eh \left[2 \frac{\partial^2 w_0}{\partial X \partial Y} \frac{\partial^2 w}{\partial X \partial Y} - \frac{\partial^2 w_0}{\partial X^2} \frac{\partial^2 w}{\partial Y^2} - \frac{\partial^2 w_0}{\partial Y^2} \frac{\partial^2 w}{\partial X^2} \right] \quad (4.1a)$$

* According to Ogibalov [1], a shell will be called: shallow if the least radius of curvature is greater by one order of magnitude than the linear dimensions, i.e., $L/R \leq 0.1$; and thin if $h/R \leq 0.01$.

$$\begin{aligned}
 D\nabla^4 w = & -q - 2 \frac{\partial^2 F}{\partial X \partial Y} \frac{\partial^2 w_0}{\partial X \partial Y} + \frac{\partial^2 F}{\partial X^2} \frac{\partial^2 w_0}{\partial Y^2} + \\
 & + \frac{\partial^2 F}{\partial Y^2} \frac{\partial^2 w_0}{\partial X^2}
 \end{aligned} \quad (4.1b)$$

where ∇^4 is the biharmonic operator, E Young's modulus, h the thickness of the shell, D the flexural rigidity, q the internal pressure and $w_0(X, Y)$ the initial shape of the shell in reference to that of a flat plate.

The usual bending moment components M_x , M_y , M_{xy} are defined in terms of the displacement function w as

$$M_x = -D \left[\frac{\partial^2 w}{\partial X^2} + \nu \frac{\partial^2 w}{\partial Y^2} \right] \quad (4.2a)$$

$$M_y = -D \left[\nu \frac{\partial^2 w}{\partial X^2} + \frac{\partial^2 w}{\partial Y^2} \right] \quad (4.2b)$$

$$M_{xy} = -D \left[(1 - \nu) \frac{\partial^2 w}{\partial X \partial Y} \right] \quad (4.2c)$$

and the membrane forces in terms of the stress function F as

$$N_x = \frac{\partial^2 F}{\partial Y^2} \quad (4.3a)$$

$$N_y = \frac{\partial^2 F}{\partial X^2} \quad (4.3b)$$

$$N_{xy} = -\frac{\partial^2 F}{\partial X \partial Y} \quad (4.3c)$$

Finally, in view of equations (4.2) and (4.3), the bending and extensional stress components become:

$$\sigma_x^{(b)} = -\frac{EZ}{(1 - \nu^2)} \left[\frac{\partial^2 w}{\partial X^2} + \nu \frac{\partial^2 w}{\partial Y^2} \right] \quad (4.4a)$$

$$\sigma_y^{(b)} = -\frac{EZ}{(1 - \nu^2)} \left[\nu \frac{\partial^2 w}{\partial X^2} + \frac{\partial^2 w}{\partial Y^2} \right] \quad (4.4b)$$

$$\tau_{xy}^{(b)} = -2GZ \left[\frac{\partial^2 w}{\partial X \partial Y} \right] \quad (4.4c)$$

and

$$\sigma_x^{(e)} = \frac{1}{h} \frac{\partial^2 F}{\partial Y^2} \quad (4.5a)$$

$$\sigma_y^{(e)} = \frac{1}{h} \frac{\partial^2 F}{\partial X^2} \quad (4.5b)$$

$$\tau_{xy}^{(e)} = - \frac{1}{h} \frac{\partial^2 F}{\partial X \partial Y} \quad (4.5c)$$

with ν being Poisson's ratio.

Because of the coupled nature of the differential equations (4.1), it becomes apparent that there exists an interaction between bending and stretching. That is, a bending load will generally produce both bending and extensional stresses, and similarly a stretching load will also induce both bending and extensional stresses. The subject of eventual concern, therefore, is that of the simultaneous stress fields produced in an initially curved sheet containing a crack.

A theoretical attack of the general problem for an arbitrary initial curvature presents formidable mathematical complexities. However, for the two simple geometries, spherical and cylindrical shells, exact solutions can be obtained in an asymptotic form. On the other hand, for other more complicated shell geometries results can be obtained by a proper superposition of these two solutions.

Spherical shell. For a shallow spherical shell the radius of curvature remains constant in all directions; therefore,

$$\frac{\partial^2 w_0}{\partial X \partial Y} = 0; \quad \frac{\partial^2 w_0}{\partial X^2} = \frac{\partial^2 w_0}{\partial Y^2} = \frac{1}{R} \quad (4.6)$$

Substituting equations (4.6) into (4.1), one recovers Reissner's equations [3]

$$\frac{Eh}{R} \nabla^2 w + \nabla^4 F = 0 \quad (4.7a)$$

$$\nabla^4 w - \frac{1}{RD} \nabla^2 F = - \frac{q}{D} \quad (4.7b)$$

Flat plate. A flat plate represents a degenerative case of a spherical cap when the radius becomes infinite; therefore,

$$\frac{\partial^2 w_0}{\partial X \partial Y} = \frac{\partial^2 w_0}{\partial X^2} = \frac{\partial^2 w_0}{\partial Y^2} = 0 \quad (4.8)$$

Substituting equation (4.8) into (4.1), one recovers the classic equations for a flat plate, i.e.,

$$\nabla^4 F = 0 \quad (4.9a)$$

$$\nabla^4 w = - \frac{q}{D} \quad (4.9b)$$

Cylindrical shell. For a shallow cylindrical shell, one of the principal radii of curvatures is infinite, while the other one is constant; therefore,

$$\frac{\partial^2 w_0}{\partial X \partial Y} = \frac{\partial^2 w_0}{\partial X^2} = 0; \quad \frac{\partial^2 w_0}{\partial Y^2} = \frac{1}{R} \quad (4.10)$$

Substituting equations (4.10) into (4.1), one recovers the equations for a shallow cylindrical shell, i.e.,

$$\frac{Eh}{R} \frac{\partial^2 w}{\partial X^2} + \nabla^4 F = 0 \quad (4.11a)$$

$$\nabla^4 w - \frac{1}{RD} \frac{\partial^2 F}{\partial X^2} = - \frac{q}{D} \quad (4.11b)$$

Other shell geometries. If one chooses the coordinate axes X and Y such that they are parallel to the principal radii of curvature*, then

$$\frac{\partial^2 w_0}{\partial X \partial Y} = 0; \quad \frac{\partial^2 w_0}{\partial X^2} = \frac{1}{R_x}; \quad \frac{\partial^2 w_0}{\partial Y^2} = \frac{1}{R_y} \quad (4.12)$$

with R_x and R_y being the principal radii of curvatures in the X and Y directions respectively.

Substituting equations (4.12) into (4.1), one finds

$$Eh \left[\frac{1}{R_y} \frac{\partial^2 w}{\partial X^2} + \frac{1}{R_x} \frac{\partial^2 w}{\partial Y^2} \right] + \nabla^4 F = 0 \quad (4.13a)$$

$$\nabla^4 w - \frac{1}{D} \left[\frac{1}{R_y} \frac{\partial^2 F}{\partial X^2} + \frac{1}{R_x} \frac{\partial^2 F}{\partial Y^2} \right] = - \frac{q}{D} \quad (4.13b)$$

* In general, when they are not parallel, equations (4.13) will contain additional terms of the form $(\partial^2 w / \partial X \partial Y)$ and $(\partial^2 F / \partial X \partial Y)$.

4.3 The stress field in a cracked spherical shell

Formulation of the Problem. Consider a portion of a thin, shallow spherical shell of constant thickness h and subjected to an internal pressure $q(X, Y)$ (see Figure 4.2). The material of the shell is assumed to be homogeneous and

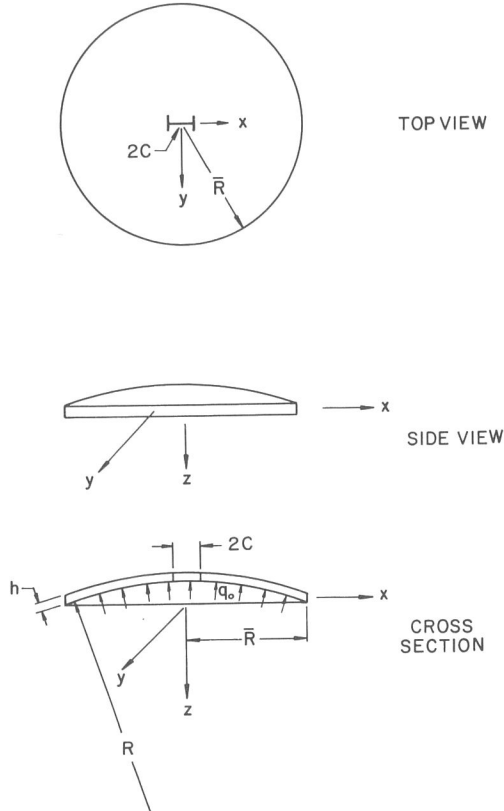


Figure 4.2. Geometrical Configurations of a Pressurized Spherical Cap

isotropic and at the apex there exists a radial cut of length $2c$ with respect to the apex. It is convenient at this point to introduce the dimensionless coordinates

$$x = \frac{X}{c}, \quad y = \frac{Y}{c}, \quad z = \frac{Z}{c} \quad (4.14)$$

in view of which the coupled differential equations governing the deflection function $w(x, y)$ and the stress function $F(x, y)$ with x and y as dimensionalized rectangular coordinates of the base plane, become

$$-\frac{Ehc^2}{R} \nabla^2 w + \nabla^4 F = 0 \quad (4.15a)$$

$$\nabla^4 w + \frac{c^2}{RD} \nabla^2 F = -c^4 \frac{q}{D} \quad (4.15b)$$

As to boundary conditions, we require that (1) on the faces of the crack, the normal moment, equivalent shear, and normal and tangential membrane forces vanish, and (2) away from the crack, the appropriate loading and support condition are satisfied.

In treating this type of problem, it is found convenient to seek the solution into two parts, the 'undisturbed' or 'particular' solution which satisfies equations (4.15) and the loading and support conditions but leaves residual forces along the crack, and the 'complementary' solution which precisely nullifies these residuals and offers no contribution far away from the crack.

However, suppose that one has already found a particular solution satisfying equations (4.15), but that there is a residual normal moment M_y , equivalent vertical shear V_y , normal in-plane stress N_y , and in-plane tangential stress N_{xy} , along the real axis $|x| < 1$, of the form:*

$$M_y^{(P)} = -\frac{D}{c^2} m_0, V_y^{(P)} = 0, N_y^{(P)} = -\frac{n_0}{c^2}, N_{xy}^{(P)} = 0 \quad (4.16)$$

where, for simplicity, we assume m_0, n_0 to be constants.**

Mathematical Statement of the Problem. Assuming therefore that a particular solution has been found, we need to find two functions of the dimensionless coordinates (x, y) , $w(x, y)$ and $F(x, y)$, such that they satisfy the homogeneous part of the differential equations (4.15) and the following boundary conditions. At $y = 0$ and $|x| < 1$:

$$M_y(x, 0) = -\frac{D}{c^2} \left[\frac{\partial^2 w}{\partial y^2} + \nu \frac{\partial^2 w}{\partial x^2} \right] = \frac{Dm_0}{c^2} = \frac{\bar{\sigma}^{(b)} h^2}{6} \quad (4.16a)$$

* For particular solutions see section 4.8.

** For m_0, n_0 non-constants, see remarks after equations (4.40).

$$V_y(x, 0) = -\frac{D}{c^2} \left[\frac{\partial^2 w}{\partial y^2} + (2 - \nu) \frac{\partial^2 w}{\partial x^2 \partial y} \right] = 0 \quad (4.16b)$$

$$N_y(x, 0) = \frac{1}{c^2} \frac{\partial^2 F}{\partial x^2} = \frac{n_0}{c^2} = h\bar{\sigma}^{(e)} \quad (4.16c)$$

$$N_{xy}(x, 0) = -\frac{1}{c^2} \frac{\partial^2 F}{\partial x \partial y} = 0 \quad (4.16d)$$

At $y = 0$ and $|x| > 1$ we must satisfy the continuity requirements, i.e.,

$$\lim_{|y| \rightarrow 0} \left[\frac{\partial^n}{\partial y^n} (w^+) - \frac{\partial^n}{\partial y^n} (w^-) \right] = 0 \quad (4.17a)$$

$$\lim_{|y| \rightarrow 0} \left[\frac{\partial^n}{\partial y^n} (F^+) - \frac{\partial^n}{\partial y^n} (F^-) \right] = 0 \quad (4.17b)$$

for $n = 0, 1, 2, 3$. Furthermore, in order to avoid infinite stresses and infinite displacements we require that the functions w and F with their first derivatives to be finite far away from the crack. These restrictions simplify the mathematical complexities of the problem considerably, and correspond to the usual expectations of the St. Venant Principle. It should be pointed out that the boundary conditions at infinity are not geometrically feasible. However if the crack is small compared to the dimensions of the shell, the approximation is reasonable.

Reduction of the System. Reissner [4] has shown that the homogeneous solution to the system of equation (4.15) can be written in the following form

$$w^{(h)} = \chi + \phi, \quad F^{(h)} = -RDc^{-2} \nabla^2 \chi + \psi \quad (4.18)$$

where ϕ and ψ are harmonic functions and χ satisfies the same differential equation as the deflection of a plate on an elastic foundation, i.e.,

$$(\nabla^4 + \lambda^4)\chi = 0 \quad (4.19)$$

with

$$\lambda^4 \equiv \frac{Ehc^4}{R^2D} \equiv \frac{12(1 - \nu^2)}{(R/h)^2} \left(\frac{c}{h} \right)^4 \quad (4.20)$$

One concludes, therefore, that the effect of the initial curvature is qualitatively equivalent to providing an elastic foundation for an initially flat

plate, such that, as the radius of curvature increases, the foundation modulus becomes weaker and weaker. This analogy has also been observed and demonstrated experimentally by Sechler and Williams [5].

Method of Solution. We construct next the following Fourier integral representations with the proper behavior at infinity

$$w(x, y \pm) = \int_0^{\infty} \{P_1 \exp [-(s^2 - i\lambda^2)^{\frac{1}{2}} |y|] + P_2 \exp [-(s^2 + i\lambda^2)^{\frac{1}{2}} |y|] + P_3 e^{-s|y|}\} \cos xs \, ds \quad (4.21a)$$

$$F(x, y \pm) = \frac{i\lambda^2 RD}{c^2} \int_0^{\infty} \{P_1 \exp [-(s^2 - i\lambda^2)^{\frac{1}{2}} |y|] - P_2 \exp [-(s^2 + i\lambda^2)^{\frac{1}{2}} |y|] + P_4 e^{-s|y|}\} \cos xs \, ds \quad (4.21b)$$

where the P_i 's are arbitrary functions of s to be determined from the boundary conditions, and the \pm signs refer to $y > 0$ and $y < 0$ respectively.

Assuming that one can differentiate under the integral sign, one finds by formally substituting equations (4.21) into the boundary conditions in equations (4.16) that:

$$\lim_{|y| \rightarrow 0} \int_0^{\infty} \{P_1(v_0 s^2 - i\lambda^2) e^{-(s^2 - i\lambda^2)^{1/2} |y|} + P_2(v_0 s^2 + i\lambda^2) e^{-(s^2 + i\lambda^2)^{1/2} |y|} + v_0 s^2 P_3 e^{-s|y|}\} \cos(xs) ds = -m_0; \quad |x| < 1 \quad (4.22a)$$

$$\pm \int_0^{\infty} \{P_1(s^2 - i\lambda^2)^{\frac{1}{2}} (v_0 s^2 + i\lambda^2) + P_2(s^2 + i\lambda^2)^{\frac{1}{2}} (v_0 s^2 - i\lambda^2) + v_0 s^3 P_3\} \cos(xs) ds = 0; \quad |x| < 1 \quad (4.22b)$$

$$\lim_{|y| \rightarrow 0} -\frac{i\lambda^2 RD}{c^2} \int_0^{\infty} \{P_1 e^{-(s^2 - i\lambda^2)^{1/2} |y|} - P_2 e^{-(s^2 + i\lambda^2)^{1/2} |y|} + P_4 e^{-s|y|}\} s^2 \cos(xs) ds = -n_0; \quad |x| < 1 \quad (4.22c)$$

and

$$\mp \frac{i\lambda^2 RD}{c^2} \int_0^{\infty} \{P_1(s^2 - i\lambda^2)^{\frac{1}{2}} - P_2(s^2 + i\lambda^2)^{\frac{1}{2}} + P_4 s\} s \sin(xs) \, ds = 0; \quad |x| < 1 \quad (4.22d)$$

where again the \mp signs refers to $y > 0$ and $y < 0$ respectively, and $v_0 = 1 - \nu$. If one, now, chooses

$$v_0 s^3 P_3 = -\{(s^2 - i\lambda^2)^{\frac{1}{2}} (v_0 s^2 + i\lambda^2) P_1 + (s^2 + i\lambda^2)^{\frac{1}{2}} (v_0 s^2 - i\lambda^2) P_2\} \quad (4.23a)$$

$$s P_4 = -\{P_1(s^2 - i\lambda^2)^{\frac{1}{2}} - P_2(s^2 + i\lambda^2)^{\frac{1}{2}}\} \quad (4.23b)$$

then equations (4.22b) and (4.22d) are satisfied automatically and equations (4.22a) and (4.22c) become, respectively

$$\int_0^{\infty} \{ [v_0 s^2 - i\lambda^2 - s^{-1}(s^2 - i\lambda^2)^{\frac{1}{2}}(v_0 s^2 + i\lambda^2)] P_1 + [v_0 s^2 + i\lambda^2 - s^{-1}(s^2 + i\lambda^2)^{\frac{1}{2}}(v_0 s^2 - i\lambda^2)] P_2 \} \cos(xs) ds = -m_0;$$

and |x| < 1 (4.24a)

$$- \frac{i\lambda^2 RD}{c^2} \int_0^{\infty} [(1 - s^{-1}(s^2 - i\lambda^2)^{\frac{1}{2}}) P_1 - (1 - s^{-1}(s^2 + i\lambda^2)^{\frac{1}{2}}) P_2] s^2 \cos(xs) ds = n_0; \quad |x| < 1 \quad (4.24b)$$

Furthermore, it can easily be shown that all the continuity conditions are satisfied if one considers the following two combinations to vanish

$$\int_0^{\infty} \frac{P_1}{s^2} (s^2 - i\lambda^2)^{\frac{1}{2}} \cos(xs) ds = 0; \quad |x| > 1 \quad (4.25a)$$

$$\int_0^{\infty} \frac{P_2}{s^2} (s^2 + i\lambda^2)^{\frac{1}{2}} \cos(xs) ds = 0; \quad |x| > 1 \quad (4.25b)$$

We have reduced, therefore, our problem to that of solving the dual integral equations (4.24) and (4.25) for the unknown functions $P_1(s)$ and $P_2(s)$.

Reduction to Singular Integral Equations. For the determination of the unknown functions $P_1(s)$ and $P_2(s)$, we reduce the problem to a set of coupled singular integral equations of the Cauchy type. This can be accomplished if one lets

$$\int_0^{\infty} \frac{P_1}{s^2} (s^2 - i\lambda^2)^{\frac{1}{2}} \cos(xs) ds = u_1(x); \quad |x| < 1 \quad (4.26a)$$

$$\int_0^{\infty} \frac{P_2}{s^2} (s^2 + i\lambda^2)^{\frac{1}{2}} \cos(xs) ds = u_2(x); \quad |x| < 1 \quad (4.26b)$$

which by Fourier inversion give

$$P_1(s^2 - i\lambda^2)^{\frac{1}{2}} = \frac{2s^2}{\pi} \int_0^1 u_1(\xi) \cos(s\xi) d\xi \quad (4.27a)$$

$$P_2(s^2 + i\lambda^2)^{\frac{1}{2}} = \frac{2s^2}{\pi} \int_0^1 u_2(\xi) \cos(s\xi) d\xi \quad (4.27b)$$

where the functions $u_1(\xi)$ and $u_2(\xi)$, due to the symmetry of the problem, are even. Next, substituting formally equations (4.27) into (4.24) one has after changing the order of integration and rearranging

$$N_y = - \frac{2i\lambda^2 RD}{\pi c^2} \int_{-1}^1 \{u_1(\xi)L_1^* - u_2(\xi)L_2^*\} d\xi \quad (4.28a)$$

$$M_y = - \frac{2D}{\pi} \int_{-1}^1 \{u_1(\xi)L_3^* + u_2(\xi)L_4^*\} d\xi \quad (4.28b)$$

where

$$L_1^* = \frac{1}{2} \int_0^\infty \frac{s^4 \exp[-(s^2 - i\lambda^2)^{\frac{1}{2}} |y|]}{(s^2 - i\lambda^2)^{\frac{1}{2}}} \cos(x - \xi) s ds - \frac{1}{2} \int_0^\infty s^3 e^{-s|y|} \cos(x - \xi) s ds \quad (4.29a)$$

$$L_2^* = \frac{1}{2} \int_0^\infty \frac{s^4 \exp[-(s^2 + i\lambda^2)^{\frac{1}{2}} |y|]}{(s^2 + i\lambda^2)^{\frac{1}{2}}} \cos(x - \xi) s ds - \frac{1}{2} \int_0^\infty s^3 e^{s|y|} \cos(x - \xi) s ds \quad (4.29b)$$

$$L_3^* = \frac{1}{2} \int_0^\infty \left\{ \frac{s^2(v_0 s^2 - i\lambda^2)}{(s^2 - i\lambda^2)^{\frac{1}{2}}} \exp[-(s^2 - i\lambda^2)^{\frac{1}{2}} |y|] - s(v_0 s^2 + i\lambda^2) e^{-s|y|} \right\} \cos(x - \xi) s ds \quad (4.29c)$$

$$L_4^* = \frac{1}{2} \int_0^\infty \left\{ \frac{s^2(v_0 s^2 + i\lambda^2)}{(s^2 + i\lambda^2)^{\frac{1}{2}}} \exp[-(s^2 + i\lambda^2)^{\frac{1}{2}} |y|] - s(v_0 s^2 - i\lambda^2) e^{-s|y|} \right\} \cos(x - \xi) s ds \quad (4.29d)$$

The integration in equations (4.29) may now be carried out explicitly by making use of the Fourier cosine transforms [6]

$$\int_0^\infty e^{-|y|s} \cos(\zeta s) ds = \frac{|y|}{p^2} \quad (4.30a)$$

$$\int_0^\infty \frac{\exp[-(s^2 + a^2)^{\frac{1}{2}} |y|]}{(s^2 + a^2)^{\frac{1}{2}}} \cos(\zeta s) ds = K_0(ap); \operatorname{Re} a > 0 \quad (4.30b)$$

and similar results obtained by differentiating them with respect to x and y . In these formulas $p^2 = \zeta^2 + |y|^2$, and K_n denotes the modified Bessel function of the third kind of order n .

The expressions in equations (4.29) then become respectively

$$2L_1^* = \frac{\partial}{\partial x} \left\{ -\frac{\lambda^2 \beta^2 \zeta}{p^4} (\zeta^2 - 3|y|^2) K_0(\lambda \beta p) \right. \\ \left. - \left[\frac{\lambda^3 \beta^3 \zeta^3}{p^3} + \frac{2\lambda \beta \zeta}{p^5} (\zeta^2 - 3|y|^2) \right] K_1(\lambda \beta p) + \frac{2\zeta}{p^4} - \frac{8\zeta |y|^2}{p^6} \right\} \quad (4.31a)$$

$$2L_2^* = \frac{\partial}{\partial x} \left\{ -\frac{\lambda^2 \alpha^2 \zeta}{p^4} (\zeta^2 - 3|y|^2) K_0(\lambda \alpha p) \right. \\ \left. - \left[\frac{\lambda^3 \alpha^3 \zeta^3}{p^3} + \frac{2\lambda \alpha \zeta}{p^5} (\zeta^2 - 3|y|^2) \right] K_1(\lambda \alpha p) + \frac{2\zeta}{p^4} - \frac{8\zeta |y|^2}{p^6} \right\} \quad (4.31b)$$

$$2L_3^* = \frac{\partial}{\partial x} \left\{ -\frac{v_0 \lambda^2 \beta^2 \zeta}{p^4} (\zeta^2 - 3|y|^2) K_0(\lambda \beta p) \right. \\ \left. - v_0 \left[\frac{\lambda^3 \beta^3 \zeta^3}{p^3} + \frac{2\lambda \beta \zeta}{p^5} (\zeta^2 - 3|y|^2) \right] K_1(\lambda \beta p) - \frac{\alpha^2 \lambda^3 \beta \zeta}{p} K_1(\lambda \beta p) \right. \\ \left. + \frac{2v_0 \zeta}{p^4} - \frac{8\zeta |y|^2 v_0}{p^6} - \frac{\alpha^2 \lambda^2 \zeta}{p^2} \right\} \quad (4.31c)$$

$$2L_4^* = \frac{\partial}{\partial x} \left\{ -\frac{v_0 \lambda^2 \alpha^2 \zeta}{p^4} (\zeta^2 - 3|y|^2) K_0(\lambda \alpha p) \right. \\ \left. - v_0 \left[\frac{\lambda^3 \alpha^3 \zeta^3}{p^3} + \frac{2\lambda \alpha \zeta}{p^5} (\zeta^2 - 3|y|^2) \right] K_1(\lambda \alpha p) - \frac{\beta^2 \lambda^3 \alpha \zeta}{p} K_1(\lambda \alpha p) \right. \\ \left. + \frac{2v_0 \zeta}{p^4} - \frac{8\zeta |y|^2 v_0}{p^6} - \frac{\beta^2 \lambda^2 \zeta}{p^2} \right\} \quad (4.31d)$$

where for simplicity we have defined $\alpha^2 = i$ and $\beta^2 = -i$. Thus, the limits, as $|y| \rightarrow 0$, of N_y and M_y are found to be respectively

$$\lim_{|y| \rightarrow 0} N_y = -\frac{2i\lambda^2 R D}{\pi c^2} \frac{d}{dx} \int_{-1}^1 \{u_1(\xi) L_1 - u_2(\xi) L_2\} d\xi \quad (4.32a)$$

$$\lim_{|y| \rightarrow 0} M_y = -\frac{2D}{\pi} \frac{d}{dx} \int_{-1}^1 \{u_1(\xi) L_3 + u_2(\xi) L_4\} d\xi \quad (4.32b)$$

where the integrals are understood to be of Cauchy principal value and

$$2L_1 \equiv -\frac{\lambda^2 \beta^2}{\zeta} K_0(\lambda \beta |\zeta|) - \left(\lambda^3 \beta^3 \frac{\zeta}{|\zeta|} + \frac{2\lambda \beta}{\zeta |\zeta|} \right) K_1(\lambda \beta |\zeta|) + \frac{2}{\zeta^3} \quad (4.33a)$$

$$2L_2 \equiv -\frac{\lambda^2 \alpha^2}{\zeta} K_0(\lambda \alpha |\zeta|) - \left(\lambda^3 \alpha^3 \frac{\zeta}{|\zeta|} + \frac{2\lambda \alpha}{\zeta |\zeta|} \right) K_1(\lambda \alpha |\zeta|) + \frac{2}{\zeta^3} \quad (4.33b)$$

$$2L_3 \equiv -\frac{v_0 \lambda^2 \beta^2}{\zeta} K_0(\lambda \beta |\zeta|) - v_0 \left(\lambda^3 \beta^3 \frac{\zeta}{|\zeta|} + \frac{2\lambda \beta}{\zeta |\zeta|} \right) K_1(\lambda \beta |\zeta|) \\ - \lambda^3 \alpha^2 \beta \frac{\zeta}{|\zeta|} K_1(\lambda \beta |\zeta|) + \frac{2v_0}{\zeta^3} - \frac{\alpha^2 \lambda^2}{\zeta} \quad (4.33c)$$

$$2L_4 \equiv -\frac{v_0 \lambda^2 \alpha^2}{\zeta} K_0(\lambda \alpha |\zeta|) - v_0 \left(\lambda^3 \alpha^3 \frac{\zeta}{|\zeta|} + \frac{2\lambda \alpha}{\zeta |\zeta|} \right) K_1(\lambda \alpha |\zeta|) \\ - \beta^2 \lambda^3 \alpha \frac{\zeta}{|\zeta|} K_1(\lambda \alpha |\zeta|) + \frac{2v_0}{\zeta^3} - \frac{\beta^2 \lambda^2}{\zeta} \quad (4.33d)$$

If we set N_y, M_y , in the limit as $|y| \rightarrow 0$, equal to $-n_0$ and $-m_0$ respectively, integrate with respect to x , then we find that they must satisfy the integral equations

$$\int_{-1}^1 \{u_1(\xi) 2L_1 - u_2(\xi) 2L_2\} d\xi = -\frac{\pi n_0 c^2}{i \lambda^2 R D} x; \quad |x| < 1 \quad (4.34a)$$

$$\int_{-1}^1 \{u_1(\xi) 2L_3 + u_2(\xi) 2L_4\} d\xi = -\pi m_0 x; \quad |x| < 1 \quad (4.34b)$$

where the kernels L_1, L_2, L_3, L_4 , have singularities of the order $1/\zeta = 1/(x - \xi)$, as can easily be seen by observing their behavior for small arguments:

$$2L_1 = -\frac{\lambda^2 \beta^2}{2(x - \xi)} + \lambda^4 \beta^4 (x - \xi) \left[\frac{5}{32} - \frac{3\gamma}{8} - \frac{3}{8} \ln \lambda \beta \frac{|x - \xi|}{2} \right] \\ + O(\lambda^6 (x - \xi)^3 \ln \lambda |x - \xi|) \quad (4.35a)$$

$$2L_2 = -\frac{\lambda^2 \alpha^2}{2(x - \xi)} + \lambda^4 \alpha^4 (x - \xi) \left[\frac{5}{32} - \frac{3\gamma}{8} - \frac{3}{8} \ln \lambda \alpha \frac{|x - \xi|}{2} \right] \\ + O(\lambda^6 (x - \xi)^3 \ln \lambda |x - \xi|) \quad (4.35b)$$

$$2L_3 = -\frac{\lambda^2 \alpha^2 (4 - v_0)}{2(x - \xi)} + \lambda^4 \beta^4 (x - \xi) \left[\frac{5v_0 - 8}{32} + \frac{4 - 3v_0}{8} \right. \\ \left. \left(\gamma + \ln \lambda \beta \frac{|x - \xi|}{2} \right) \right] + O(\lambda^6 (x - \xi)^3 \ln \lambda |x - \xi|) \quad (4.35c)$$

$$2L_4 = -\frac{\lambda^2 \beta^2 (4 - v_0)}{2(x - \xi)} + \lambda^4 \alpha^4 (x - \xi) \left[\frac{5v_0 - 8}{32} + \frac{4 - 3v_0}{8} \right]$$

$$\left(\gamma + \ln \frac{\lambda \alpha |x - \xi|}{2} \right) + O(\lambda^6 (x - \xi)^3 \ln \lambda |x - \xi|) \quad (4.35d)$$

We require, therefore, that the solutions $u_1(x)$, $u_2(x)$ be Hölder continuous for some positive Hölder indices μ_1 and μ_2 for all x in the closed interval $[-1, 1]$. Thus in particular, $u_1(x)$, $u_2(x)$ are to be bounded near the ends of the crack.

However, because of the complicated nature of the kernels L_i , an exact solution for the unknown functions $u_1(x)$ and $u_2(x)$ is extremely difficult. On the other hand, for most practical applications the parameter λ attains small values as follows from the definition of λ , namely

$$\lambda = \frac{[12(1 - \nu^2)]^{\frac{1}{2}}}{(R/h)^{\frac{1}{2}}} (c/h) = [12(1 - \nu^2)]^{\frac{1}{2}} (c/R) (R/h)^{\frac{1}{2}} \quad (4.36)$$

It is clear that λ is small for large ratios of R/h and small crack lengths. As a practical matter, if we consider crack lengths less than one tenth of the periphery, i.e., $2c < 2\pi R/10$, and for $R/h < 10^3$ a corresponding upper bound for λ can be obtained, namely $\lambda < 20$. Thus the range of λ becomes $0 < \lambda < 20$ and for most practical cases is between 0 and 2, depending upon the size of the crack.

Solution for Small λ . For the simple case $\lambda = 0$, the problem reduces to that of a flat sheet under applied bending and stretching loads, the solution of which has been investigated by many authors. For example, the problem for both bending and stretching for an orthotropic plate, containing a finite crack, was investigated by Ang and Williams [7] and a solution was obtained by means of dual integral equations. It can easily be shown* that the dual integral equations can be transformed to two singular integral equations of the type (4.34) with simpler kernels. Furthermore, these are not coupled and the solutions can easily be obtained as in § 47 of [9]. Without going into the details they are found to be of the form $A(1 - \xi^2)^{\frac{1}{2}}$, where A is a constant.

Similarly, the solution for an initially curved sheet must, in the limit, check the above result and because $u_1(\xi)$ and $u_2(\xi)$ are in particular to be bounded near the ends of the crack, it is reasonable to assume solutions of the form**

$$u_1(\xi) = (1 - \xi^2)^{\frac{1}{2}} [A_0 + \lambda^2 A_1 (1 - \xi^2) + \dots]; \quad |\xi| < 1 \quad (4.37a)$$

* See Noble [8].

** In fact, one can show [10] that this is precisely the form of the asymptotic solution for small λ .

$$u_2(\xi) = (1 - \xi^2)^{\frac{1}{2}} [B_0 + \lambda^2 B_1 (1 - \xi^2) + \dots]; \quad |\xi| < 1 \quad (4.37b)$$

where the coefficients $A_0, A_1, \dots, B_0, B_1, \dots$ can be functions of λ but not of ξ .

Substituting equations (4.31) into (4.34), and making use of the relation

$$\int_{-1}^1 (1 - \xi^2)^{\frac{1}{2}} (x - \xi) \ln \frac{\lambda \alpha |x - \xi|}{2} d\xi = \frac{\pi}{4} \left(1 + \ln \frac{\lambda^2 \alpha^2}{16} \right) x + \frac{\pi}{6} x^3 \quad (4.38)$$

we find by equating coefficients that*

$$\begin{aligned} A_0 = & \frac{n_0 c^2}{\lambda^4 R D} \left\{ 1 + \frac{\pi \lambda^2}{16} \frac{8 - 3\nu_0}{4 - \nu_0} + \frac{\lambda^2 \alpha^2}{4 - \nu_0} \left(\frac{8 - 7\nu_0}{32} + \frac{4 - 3\nu_0}{8} \gamma \right) \right. \\ & \left. + \frac{\lambda^2 \alpha^2}{16} \frac{4 - 3\nu_0}{4 - \nu_0} \ln \frac{\lambda^2 \alpha^2}{16} \right\} + \frac{m_0}{\lambda^2 \alpha^2 (4 - \nu_0)} \\ & \left\{ 1 + \frac{\pi \lambda^2}{16} \frac{8 - 3\nu_0}{4 - \nu_0} + \lambda^2 \alpha^2 \left(\frac{7}{32} + \frac{3\gamma}{8} \right) + \frac{3}{16} \lambda^2 \alpha^2 \left(1 + \ln \frac{\lambda^2 \alpha^2}{16} \right) \right\} \\ & + O(\lambda^2 \ln \lambda) \end{aligned} \quad (4.39a)$$

$$\begin{aligned} B_0 = & \frac{n_0 c^2}{\lambda^4 R D} \left\{ 1 + \frac{\lambda^2 \pi}{16} \frac{8 - 3\nu_0}{4 - \nu_0} + \frac{\lambda^2 \beta^2}{4 - \nu_0} \left(\frac{8 - 7\nu_0}{32} + \frac{4 - 3\nu_0}{8} \lambda \right) \right. \\ & \left. + \frac{\lambda^2 \beta^2}{16} \frac{4 - 3\nu_0}{4 - \nu_0} \ln \frac{\lambda^2 \beta^2}{16} \right\} + \frac{m_0}{\lambda^2 \beta^2 (4 - \nu_0)} \left\{ 1 + \frac{\lambda^2 \pi}{16} \frac{8 - 3\nu_0}{4 - \nu_0} \right. \\ & \left. + \lambda^2 \beta^2 \left(\frac{7}{32} + \frac{3\gamma}{8} \right) + \frac{3}{16} \lambda^2 \beta^2 \left(1 + \ln \frac{\lambda^2 \beta^2}{16} \right) \right\} + O(\lambda^2 \ln \lambda) \end{aligned} \quad (4.39b)$$

It should be pointed out that if coefficients A_0, B_0 of higher accuracy are desired, say up to order λ^{2n} , then it is necessary to solve an $n \times n$ algebraic system. In effect, this is a method of successive approximations for which the question of convergence is investigated in Reference [10].

It thus appears that for $\lambda < \lambda^*$ the power series solutions of the form

$$u_1^{(N)}(\xi) = (1 - \xi^2)^{\frac{1}{2}} \sum_{n=0}^N A_n \lambda^{2n} (1 - \xi^2)^n, \quad (4.40a)$$

$$u_2^{(N)}(\xi) = (1 - \xi^2)^{\frac{1}{2}} \sum_{n=0}^N B_n \lambda^{2n} (1 - \xi^2)^n, \quad (4.40b)$$

* For brevity, in this analysis we will restrict ourselves to terms up to $O(\lambda^2)$.

in the limit as $N \rightarrow \infty$, will converge to the exact solutions* $u_1(\xi)$ and $u_2(\xi)$ of the integral equations (4.34). However, since most particular solutions will give us a non-uniform residual moment and normal membrane stress along the crack, it is only natural to ask how the solution changes. Suppose for $|x| < 1$, we expand m_0 and n_0 in the form $\sum_n a_n x^{2n}$ (even powers because of the symmetry of the problem), then our previous method of solution will still be applicable. And as can easily be seen from equations (4.34), although the coefficients A_n, B_n in this case may change, the character of the solution will still remain the same. Finally, because we desire to focus our attention upon the singular stresses around the neighborhood of the crack point, we need only to compute coefficients A_0 and B_0 .

Alternate Method of Solution. It is also possible to solve the coupled dual integral equations directly by using a method which was developed by the author some time ago [11] and is parallel to the previous method. Thus motivated by equations (4.25) and (4.26), one assumes the unknown functions P_1 and P_2 in the form

$$\frac{P_1(s^2 - i\lambda^2)^{\frac{1}{2}}}{s^2} = \sum_{k=0}^{\infty} A_k \frac{J_{k+1}(s)}{(s)^{k+1}} \quad (4.41a)$$

and

$$\frac{P_2(s^2 + i\lambda^2)^{\frac{1}{2}}}{s^2} = \sum_{k=0}^{\infty} B_k \frac{J_{k+1}(s)}{(s)^{k+1}} \quad (4.41b)$$

where the coefficients A_k and B_k are constants to be determined.

The advantage of such a form is that equations (4.25) are automatically satisfied and furthermore,

$$u_1(x) = \int_0^{\infty} \frac{P_1}{s^2} (s^2 - i\lambda^2)^{\frac{1}{2}} \cos(xs) ds = \sum_{k=0}^{\infty} A_k \frac{\sqrt{\pi}}{2^{k+1} \Gamma(k + \frac{3}{2})} (1 - x^2)^{k + \frac{1}{2}} \quad (4.42a)$$

and

$$u_2(x) = \int_0^{\infty} \frac{P_2}{s^2} (s^2 + i\lambda^2)^{\frac{1}{2}} \cos(xs) ds = \sum_{k=0}^{\infty} B_k \frac{\sqrt{\pi}}{2^{k+1} \Gamma(k + \frac{3}{2})} (1 - x^2)^{k + \frac{1}{2}} \quad (4.42b)$$

In general, the functions u_i , have some physical meaning. For example, in this case their algebraic combination represents the crack opening displace-

* This matter is discussed at same length in [10].

ment and as a result such an expansion is plausible.

It follows that equations (4.24) take the forms

$$\begin{aligned} & \sum_{k=0}^{\infty} \int_0^{\infty} \left\{ \left[\frac{v_0 s^4 - i\lambda^2 s^2}{(s^2 - i\lambda^2)^{\frac{1}{2}}} - s(v_0 s^2 + i\lambda^2) \right] A_k \right. \\ & \left. + \left[\frac{v_0 s^4 + i\lambda^2 s^2}{(s^2 + i\lambda^2)^{\frac{1}{2}}} - s(v_0 s^2 - i\lambda^2) \right] B_k \right\} \frac{J_{k+1}(s)}{(s)^{k+1}} \cos(xs) ds \\ & = -m_0; \quad |x| < 1 \end{aligned} \quad (4.43a)$$

and

$$\begin{aligned} & \sum_{k=0}^{\infty} \int_0^{\infty} \left\{ \left[\frac{s^2}{(s^2 - i\lambda^2)^{\frac{1}{2}}} - s \right] A_k - \left[\frac{s^2}{(s^2 + i\lambda^2)^{\frac{1}{2}}} - s \right] B_k \right\} \\ & s^2 \frac{J_{k+1}(s)}{(s)^{k+1}} \cos(xs) ds = n_0; \quad |x| < 1 \end{aligned} \quad (4.43b)$$

Multiplying, subsequently, both sides by

$$\frac{(1-x^2)^{j+\frac{1}{2}}}{2^j \Gamma(j+\frac{3}{2}) \sqrt{\pi}}$$

and integrating with respect to x from 0 to 1 one finds

$$\sum_{k=0}^{\infty} \{A_k G_{k,j}(\lambda; i) + B_k G_{k,j}(\lambda; -i)\} = -m_0 H_j; \quad j = 0, 1, 2, \dots \quad (4.44a)$$

and

$$\sum_{k=0}^{\infty} \{A_k F_{k,j}(\lambda; i) - B_k F_{k,j}(\lambda; -i)\} = n_0 H_j; \quad j = 0, 1, 2, \dots \quad (4.44b)$$

where for simplicity we have made the following definitions

$$G_{k,j}(\lambda; i) = \int_0^{\infty} \left\{ \frac{v_0 s^4 - i\lambda^2 s^2}{(s^2 - i\lambda^2)^{\frac{1}{2}}} - s(v_0 s^2 + i\lambda^2) \right\} \frac{J_{k+1}(s)}{(s)^{k+1}} \frac{J_{j+1}(s)}{(s)^{j+1}} ds \quad (4.45a)$$

$$F_{k,j}(\lambda; i) = - \int_0^{\infty} s^3 \left(1 - \frac{s}{(s^2 - i\lambda^2)^{\frac{1}{2}}} \right) \frac{J_{k+1}(s)}{(s)^{k+1}} \frac{J_{j+1}(s)}{(s)^{j+1}} ds \quad (4.45b)$$

and

$$H_j = - \frac{1}{2^{j+1} (j+1)!} \quad (4.46)$$

Equations (4.44) now represent two infinite systems of algebraic equations which are to be solved for the unknown coefficients* A_k and B_k . Such systems have been studied extensively and the questions of existence and uniqueness of the solution are discussed in reference [13].

As a practical matter now, if one addresses himself to the major contribution of the solution, which comes primarily from the terms with $k = j = 0$, and uses the following integral approximation

$$\int_0^\infty s \left\{ 1 - \frac{s}{(s^2 + \beta^2)^{\frac{1}{2}}} \right\} \left\{ \frac{J_1(s)}{(s)} \right\}^2 ds \simeq \int_0^\infty s \frac{(\beta^2/2)}{s^2 + (\beta^2/2)} \left\{ \frac{J_1(s)}{(s)} \right\}^2 ds$$

$$= \left(\frac{1}{2} \right) \{ 1 - 2I_1(\beta/\sqrt{2}) K_1(\beta/\sqrt{2}) \}, \quad (4.47)$$

then

$$A_0 \simeq - \frac{m_0}{2\Delta} F_{0,0}(\lambda; -i) + \frac{n_0}{2\Delta} G_{0,0}(\lambda; -i) \quad (4.48a)$$

$$B_0 \simeq - \frac{m_0}{2\Delta} F_{0,0}(\lambda; i) - \frac{n_0}{2\Delta} G_{0,0}(\lambda; i) \quad (4.48b)$$

in which Δ is given by

$$\Delta \simeq F_{0,0}(\lambda; -i) G_{0,0}(\lambda; i) + F_{0,0}(\lambda; i) G_{0,0}(\lambda; -i) \quad (4.49)$$

Furthermore, in view of the approximation (4.47), one has

$$F_{0,0}(\lambda; i) = + \frac{i\lambda^2}{2} I_1(e^{-i\pi/4} \lambda/\sqrt{2}) K_1(e^{-i\pi/4} \lambda/\sqrt{2}) \quad (4.50a)$$

$$G_{0,0}(\lambda; +i) = \nu_0 F_{0,0}(\lambda; +i) + \frac{i\lambda^2}{2} \{ 1 - 2I_1(e^{-i\pi/4} \lambda/\sqrt{2}) K_1(e^{-i\pi/4} \lambda/\sqrt{2}) \} - i\lambda^2 \quad (4.50b)$$

It is clear now from the above, that the general expressions for the coefficients A_0 and B_0 are complicated series expressions involving the modified Bessel functions I_n and K_n . As complicated as they may seem, the use of an electronic computer makes the work a routine.

* In the field of fracture mechanics it is only necessary to compute the first coefficients A_0 and B_0 for only the first term of the series in equations (4.41) lead to the well known [12] $1/\sqrt{r}$ stress singular behavior ahead of the crack tip.

Determination of w and F . In view of equations (4.27), (4.37) to (4.39) and the relation

$$\int_0^\infty s^{-\mu} J_\mu(as) \cos(xs) ds = \begin{cases} \sqrt{\pi(2a)^{-\mu}} [\Gamma(\mu + \frac{1}{2})]^{-1} (a^2 - x^2)^{\mu - \frac{1}{2}}; & 0 < x < a; \operatorname{Re} \mu > -\frac{1}{2} \\ 0; & a < x < \infty; \operatorname{Re} \mu > -\frac{1}{2} \end{cases} \quad (4.51)$$

which can be found on page 44 of [6], we have:

$$P_1(s) = \frac{s}{(s^2 - i\lambda^2)^{\frac{1}{2}}} \left\{ A_0 J_1(s) + 3\lambda^2 A_1 \frac{J_2(s)}{s} + O(\lambda^4) \right\} \quad (4.52a)$$

$$P_2(s) = \frac{s}{(s^2 + i\lambda^2)^{\frac{1}{2}}} \left\{ B_0 J_1(s) + 3\lambda^2 B_1 \frac{J_2(s)}{s} + O(\lambda^4) \right\} \quad (4.52b)$$

$$P_3(s) = - (A_0 + B_0) J_1(s) - 3\lambda^2 (A_1 + B_1) \frac{J_2(s)}{s} - \frac{i\lambda^2}{v_0 s^2} (A_0 - B_0) J_1(s) + O(\lambda^4) \quad (4.52c)$$

$$P_4(s) = - (A_0 - B_0) J_1(s) - 3\lambda^2 (A_1 - B_1) s^{-1} J_2(s) + O(\lambda^4) \quad (4.52d)$$

Therefore a substitution of the above relations into equations (4.21) will determine the bending deflection w and membrane stress function F . Furthermore, the corresponding integrals will converge and the differentiations under the integral sign are also justified at least for $y \neq 0$. The values of the derivatives at $y = 0$ and $|x| < 1$ can be obtained by a proper limiting process.

The Stress Field. Without going into the details, the stress distribution around the crack tip for a symmetrical loading* is found to be:

Extensional stresses: through the thickness

$$\sigma_x^{(e)} = \frac{k_1^{(e)}}{(2r)^{\frac{1}{2}}} \cos(\theta/2) [1 - \sin(\theta/2) \sin(3\theta/2)] \quad (4.53a)$$

$$\sigma_x^{(e)} = \frac{k_1^{(e)}}{(2r)^{\frac{1}{2}}} \cos(\theta/2) [1 + \sin(\theta/2) \sin(3\theta/2)] \quad (4.53b)$$

* The antisymmetric loading case will be discussed later.

$$\sigma_{xy}^{(e)} = \frac{k_1^{(e)}}{(2r)^{\frac{3}{2}}} \cos(\theta/2) \sin(\theta/2) \cos(3\theta/2) \quad (4.53c)$$

Bending stresses: on the 'tension side' of the shell

$$\sigma_x^{(b)} = -\frac{k_1^{(b)}}{(2r)^{\frac{3}{2}}} \kappa [3 \cos(\theta/2) + \cos(5\theta/2)] \quad (4.54a)$$

$$\sigma_y^{(b)} = \frac{k_1^{(b)}}{(2r)^{\frac{3}{2}}} \kappa \left[\cos(5\theta/2) + \frac{11+5\nu}{1-\nu} \cos(\theta/2) \right] \quad (4.54b)$$

$$\sigma_{xy}^{(b)} = \frac{k_1^{(b)}}{(2r)^{\frac{3}{2}}} \kappa \left[\sin(5\theta/2) + \left(\frac{7+\nu}{1+\nu} \right) \sin(\theta/2) \right] \quad (4.54c)$$

where ν is Poisson's ratio and (r, θ) are the polar coordinates around the crack tip. In general, the stress intensity factors $k_1^{(e)}$ and $k_1^{(b)}$ are functions of crack size, geometry of the shell, material properties and loading characteristics. In this case, they are related to the coefficients A_0 and B_0 by the expressions

$$k_1^{(e)} = \frac{\lambda^4 RD}{2hc^4} (A_0 + B_0) \sqrt{c} \quad (4.55a)$$

$$k_1^{(b)} = \frac{iEh\lambda^2}{4(1-\nu^2)c^2} (A_0 - B_0) (3 + \nu) \sqrt{c} \quad (4.55b)$$

Thus, in view of equations (4.39), the stress intensity factors

$$k_1^{(e)} = \bar{\sigma}^{(e)} \sqrt{c} \left\{ 1 + \frac{3\pi}{32} \lambda^2 \right\} + \bar{\sigma}^{(b)} \sqrt{c} \frac{(\lambda^2)(1-\nu^2)^{\frac{1}{2}}}{3^{\frac{1}{2}}} \left\{ \frac{7}{32} + \frac{3}{8} \left(\lambda + \ln \frac{\lambda}{4} \right) \right\} + O(\lambda^4 \ln \lambda) \quad (4.56)$$

and

$$k_1^{(b)} = -\bar{\sigma}^{(e)} \frac{\lambda^2(3^{\frac{1}{2}})\sqrt{c}}{(1-\nu^2)^{\frac{1}{2}}(3+\nu)} \left\{ \frac{1+7\nu}{32} + \frac{1+3\nu}{8} \left(\gamma + \ln \frac{\lambda}{4} \right) \right\} - \bar{\sigma}^{(b)} \sqrt{c} \left\{ 1 + \frac{1+3\nu}{3+\nu} \frac{\pi\lambda^2}{32} \right\} + O(\lambda^4 \ln \lambda) \quad (4.57)$$

are obtained.

The reader should be cautioned for equations (4.56) and (4.57) represent exact asymptotic expansions up to $O(\lambda^2)$ terms. Consequently, they are good approximations for $0 \leq \lambda < 1$. For larger values of λ , one must also include

higher order terms in order to guarantee convergence. This can be done by either of the two methods discussed previously and the aid of a computer. For example, the numerical solution of the system of equation (4.44) leads to a numerical result that may well be approximated within a 5% error by the simple relation*

$$k_1^{(e)} \simeq \sigma^{(e)} \sqrt{c(1 + 0.466 \lambda^2)^{\frac{1}{2}}} \quad (4.58)$$

which is valid for all values of λ .

In view of the above, one may conjecture that in an initially curved sheet,

1. the stresses are proportional to $(c/r)^{\frac{1}{2}}$,
2. the stresses have the same angular distribution as that of a flat plate,
3. the stress intensity factors are functions of the shell geometry and, in the limit, we recover the flat plate,
4. the stresses include interaction terms for bending and stretching.

A typical term for a spherical shell is

$$\frac{\sigma_{\text{shell}}}{\sigma_{\text{plate}}} \simeq 1 + \frac{c^2}{Rh} \left(a_1 + b_1 \ln \frac{c}{(Rh)^{\frac{1}{2}}} \right) + O\left(\frac{1}{R^2}\right) \quad (4.59)$$

where the expression inside the parenthesis is a positive quantity. One concludes, therefore, that a spherical initial curvature, in reference to that of a flat sheet, is to increase the stresses in the neighborhood of the crack tip and, as a result, reduce its resistance to fracture initiation.

It should be emphasized that classical bending theory has been used in deducing the foregoing results. Hence it is inherent that only the Kirchoff equivalent shear free condition is satisfied along the crack [15], and not the vanishing of both individual shearing stresses. While outside the local region the stress distribution should be accurate, one might expect the same type of discrepancy to exist near the crack point as that found by Knowles and Wang [16] in comparing Kirchoff and Reissner bending results for a flat plate. In this case the order of the stress singularity remained unchanged but the angular distribution around the crack changed so as to precisely be the same as that due to solely extensional loading.

Recently, Sih and Hagendorf [17] investigated this matter further by deriving an improved theory of shallow shells which incorporates the effect of a transverse shear deformation. As expected, their results** showed that

* For the prediction of failures in pressurized vessels [14] the contributions of $k_1^{(b)}$ are negligible in comparison to those of $k_1^{(e)}$.

** See chapter 6.

classic theory cannot adequately predict the exact angular dependence of the bending stresses in the vicinity of a crack. However, in general, these bending stresses are so small when compared to the extensional stresses that can be neglected. On the other hand, for very long cracks such contributions become significant and consequently may no longer be neglected. Unfortunately, in such cases bulging effects become extremely important and any theory, whether classic or shear, is inadequate.

In-plane Shear Load. If on the other hand, the residual loads, i.e., equation (4.16), are of the form

$$M_y^{(P)} = 0, V_y^{(P)} = 0, N_y^{(P)} = 0, N_{xy}^{(P)} = -\frac{I_0}{c^2} \quad (4.60)$$

then the solution can be constructed in a similar manner [10] and the results are

Extensional stresses: through the thickness:

$$\sigma_x^{(e)} = -\frac{k_2^{(e)}}{(2r)^{\frac{3}{2}}} \sin(\theta/2) [2 + \cos(\theta/2) \cos(3\theta/2)] \quad (4.61a)$$

$$\sigma_y^{(e)} = \frac{k_2^{(e)}}{(2r)^{\frac{3}{2}}} \sin(\theta/2) \cos(\theta/2) \cos(3\theta/2) \quad (4.61b)$$

$$\sigma_{xy}^{(e)} = \frac{k_2^{(e)}}{(2r)^{\frac{3}{2}}} \cos(\theta/2) [1 - \sin(\theta/2) \sin(3\theta/2)] \quad (4.61c)$$

Bending stresses: on the 'tension side' of the shell:

$$\sigma_x^{(b)} = \frac{k_2^{(b)}}{(2r)^{\frac{3}{2}}} \kappa \left[\sin(5\theta/2) - \left(\frac{9+7\nu}{1-\nu} \right) \sin(\theta/2) \right] \quad (4.62a)$$

$$\sigma_y^{(b)} = \frac{k_2^{(b)}}{(2r)^{\frac{3}{2}}} \kappa [\sin(\theta/2) - \sin(5\theta/2)] \quad (4.62b)$$

$$\sigma_{xy}^{(b)} = \frac{k_2^{(b)}}{(2r)^{\frac{3}{2}}} \kappa \left[\left(\frac{3\nu+5}{1-\nu} \right) \cos(\theta/2) - \cos(5\theta/2) \right] \quad (4.62c)$$

where the stress intensity factors $k_2^{(e)}$ and $k_2^{(b)}$ are given by

$$k_2^{(e)} = -\tau^{(e)} \sqrt{c} \left\{ 1 + \frac{\pi\lambda^2}{32} + O(\lambda^4 \ln \lambda) \right\} \quad (4.63a)$$

$$k_2^{(b)} = -\bar{\tau}^{(e)} \frac{\sqrt{3(3+v)}}{2(1-v^2)^{\frac{3}{2}}} \lambda^2 \left\{ \frac{7+v-4(5-v)\gamma}{16(1-v)} - \frac{5-v}{4(1-v)} \ln \frac{\lambda}{4} \right. \\ \left. + O(\lambda^2 \ln \lambda) \right\} \quad (4.63b)$$

with

$$\bar{\tau}^{(e)} = \frac{t_0}{hc^2} \quad (4.64)$$

In the limit, as $\lambda \rightarrow 0$ one recovers precisely the results of references [18] and [15]. Here again the results are correct up to $O(\lambda^4)$ terms and as a result they are only good approximations for $0 \leq \lambda < 1$.

Effect of Transverse Vibrations. In addition to the usual external applied loads, pressure vessels are frequently also subjected to vibrations. Consequently, an investigation was carried out in order to assess analytically what effect, if any, do vibrations have on the mechanism of fracture. The analysis has shown [19] that in general, transverse vibrations reduce the stress intensity factor. However, when the forcing frequency ω approaches the natural frequency of the uncracked shell, the stress intensity factor increases without bound. This phenomenon, coupled with the usual $1/\sqrt{r}$ singular behavior, causes the pressure vessel to fail at nominal values even lower than the yield stress.

Thus, without going into the mathematical details [19], the stress intensity factors for a residual load* of the form

$$M_y^{(P)} = -\frac{D}{c^2} m_0 \cos(\omega t + \phi), \quad V_y^{(P)} = 0, \quad (4.65a)$$

$$N_y^{(P)} = -\frac{n_0}{c^2} \cos(\omega t + \phi), \quad N_{xy}^{(P)} = 0, \quad (4.65b)$$

are

case (i) $\lambda^4 \geq 0$:

$$k_1^{(e)} = \sqrt{c} \left\{ \frac{n_0}{hc^2} + \frac{m_0 E}{(3+v)R} \left[\frac{7}{32} + \frac{3}{8} \left(\gamma + \ln \frac{\lambda}{4} \right) \right] + O(\lambda^4 \ln \lambda) \right\} \cos(\omega t + \phi) \quad (4.66a)$$

* See equation (4.16).

$$k_1^{(b)} = \left\{ -\frac{\lambda^4 R n_0 \sqrt{c}}{2(1-v^2)c^4} \left[\frac{1+7\nu}{32} + \frac{1+3\nu}{8} \left(\gamma + \ln \frac{\lambda}{4} \right) \right] + \frac{m_0 E h \sqrt{c}}{2(1-v^2)c^4} + O(\lambda^4 \ln \lambda) \right\} \cos(\omega t + \phi) \quad (4.66b)$$

case (ii) $\lambda^4 < 0$:

$$k_1^{(e)} = \sqrt{c} \left\{ \frac{n_0}{hc} \left[1 + \frac{3\pi}{32} \lambda^2 \right] + \frac{m_0 E}{R(3+\nu)} \left[\frac{7}{32} + \frac{3}{8} \left(\gamma + \ln \frac{\lambda}{4} \right) \right] + O(\lambda^4 \ln \lambda) \right\} \cos(\omega t + \phi) \quad (4.67a)$$

$$k_1^{(b)} = \left\{ -\frac{\lambda^4 R n_0 \sqrt{c}}{2(1-v^2)c^4} \left[\frac{1+7\nu}{32} + \frac{1+3\nu}{8} \left(\gamma + \ln \frac{\lambda}{4} \right) \right] + \frac{m_0 E h \sqrt{c}}{2(1-v^2)c^4} \left[1 + \frac{\pi \lambda^2}{32} \frac{1+3\nu}{3+\nu} \right] + O(\lambda^4 \ln \lambda) \right\} \cos(\omega t + \phi) \quad (4.67b)$$

where

$$\lambda^4 \equiv \frac{\rho h c^4}{D} \omega^2 - \frac{E h c^4}{R^2 D}, \quad (4.68)$$

ω the forcing frequency and ρ the density of the material.

From these results, the following special limiting cases of practical interest can be examined:

1. If $\omega \rightarrow 0$ and $R \neq \infty$, the stresses of a non-vibrating cracked spherical shell are recovered and coincide with those obtained in [10].
2. If $\omega \neq 0$ and $R \rightarrow \infty$, we recover the vibrating cracked plate expressions in [20].
3. If $\omega = 0$ and $R \rightarrow \infty$, the stresses of a flat sheet are recovered and coincide with those obtained previously for bending [15] and extension [18].
4. If $\lambda \rightarrow 0$, i.e., when the forcing frequency reaches the natural frequency $(E/\rho)^{\frac{1}{2}} (1/R)$ of the uncracked shell, the extensional stress intensity factor becomes infinite.

As a practical matter, it is of some value to compare the dynamic with the static stress along the line of crack prolongation. For $c = 1$ in., $h = 0.1$ in., $R = 32.6$ in., $\nu = 1/3$, $E = 16 \times 10^6$ psi, $\rho = 0.315$ lbf/in.³.

(i) for $n_0 \neq 0$, $m_0 = 0$:

$$\frac{\sigma_{ydynamic}}{\sigma_{ystatic}} = \begin{cases} \left[0.67(1 + 0.29\lambda^2) - 1.24\lambda^4 \left(0.25 + 0.13 \ln \frac{\lambda^2}{16} \right) \right] \\ \cos(\omega t + \phi); \lambda^4 < 0 \\ \left[0.67 - 1.24\lambda^2 \left(0.25 + 0.13 \ln \frac{\lambda^2}{16} \right) \right] \cos(\omega t + \phi); \\ \lambda^4 > 0 \end{cases}$$

(ii) for $n_0 = 0, m_0 \neq 0$:

$$\frac{\sigma_{ydynamic}}{\sigma_{ystatic}} = \begin{cases} \left[0.87(1 + 0.18\lambda^2) + 0.14 \left(0.43 + 0.19 \ln \frac{\lambda^2}{16} \right) \right] \\ \cos(\omega t + \phi); \lambda^4 < 0 \\ \left[0.87 + 0.14 \left(0.43 + 0.19 \ln \frac{\lambda^2}{16} \right) \right] \cos(\omega t + \phi); \lambda^4 > 0 \end{cases}$$

where

$$\lambda^4 = 2.1 \times 10^{-5} \omega^2 - 1$$

The plots of the ratio

$$I = \frac{\sigma_{ydynamic}}{\sigma_{ystatic} \cos(\omega t + \phi)}$$

for various values of ω are given in Figures 4.3 and 4.4.

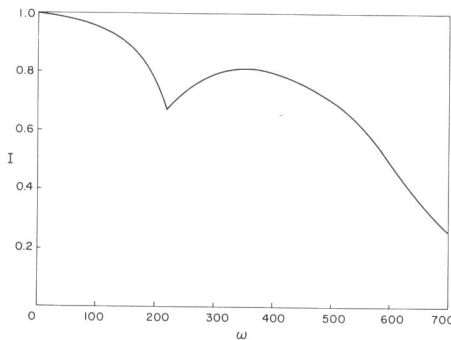


Figure 4.3. Ratio of Dynamic and Static Stresses *vs* ω for $m_0 = 0$

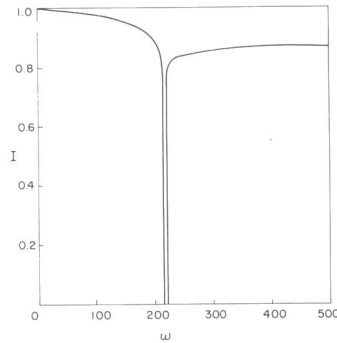


Figure 4.4. Ratio of Dynamic and Static Stresses *vs* ω for $n_0 = 0$

4.4 The stress field in a cracked plate

The problem of a flat plate containing a finite crack has been investigated by many authors for various types of loadings and the results are reported in other chapters of this volume. The solution, however, for an infinite plate (see Figure 4.5) may also be obtained from that of a spherical cap by simply

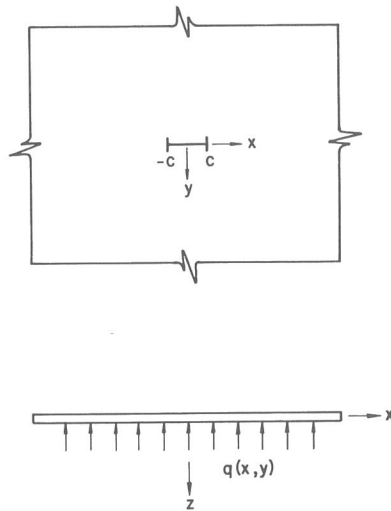


Figure 4.5. Cracked Plate Subjected to a Lateral Load q

letting $R \rightarrow \infty$ or $\lambda \rightarrow 0$. Thus the stress field around the crack tip is given by equations (4.53) and (4.54) where the stress intensity factors now are

$$k_1^{(e)} = \bar{\sigma}^{(e)} \sqrt{c} \quad (4.69a)$$

$$k_1^{(b)} = -\bar{\sigma}^{(b)} \sqrt{c} \quad (4.69b)$$

4.5 The stress field in a cracked cylindrical shell

For a cylindrical shell, one of the principal radii of curvature is infinite and the other constant. It appears therefore that this geometric simplicity leads to rather straightforward analytical solutions. However, the fact that the curvature varies between zero and a constant as one considers different angular positions—say around the point of a crack which is aligned parallel to the cylinder axis—more than obviates the initial geometric simplification and therefore increases the mathematical complexities considerably. For this reason, Sechler and Williams [5] suggested an approximate equation, based upon the behavior of a beam on an elastic foundation, and were able

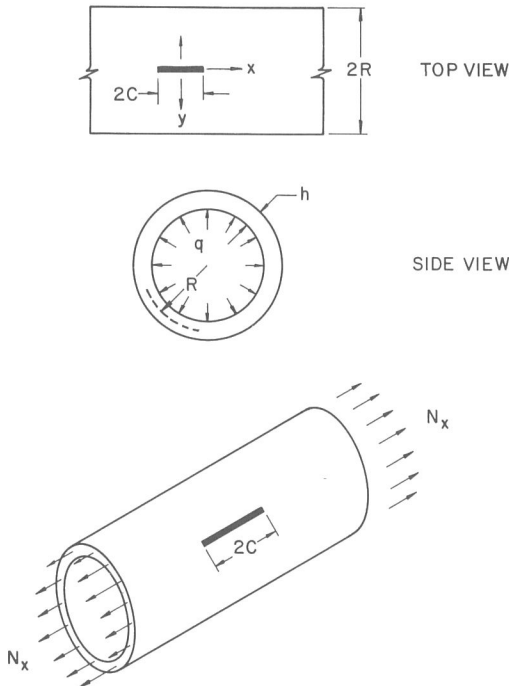


Figure 4.6. Geometry and Coordinates of an Axially Cracked Cylindrical Shell Under Uniform Axial Extension N_x and Internal Pressure q_0

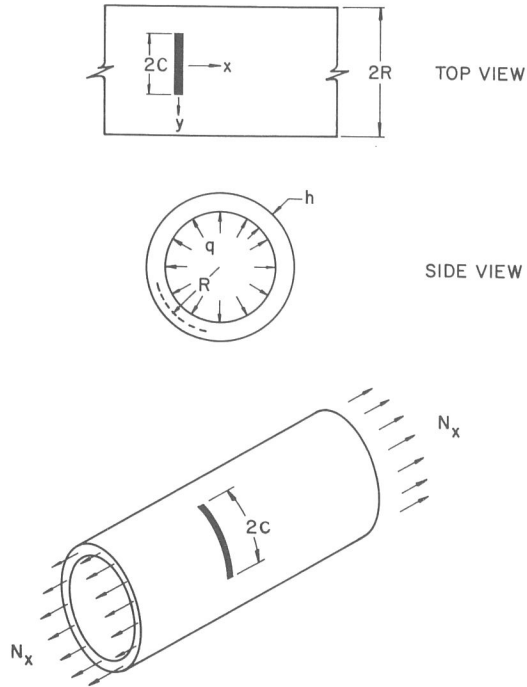


Figure 4.7. Geometry and Coordinates of a Peripherally Cracked Cylindrical Shell Under Uniform Axial Extension N_x and Internal Pressure q_0

to obtain a reasonable agreement with the experimental results. Subsequently, using the method of section 2, the author investigated this problem in a more sophisticated manner and the details for an axial and a peripheral crack (see Figures 4.6 and 4.7) can be found in references [21] and [22], respectively.

Again, omitting the mathematical details, the stresses around the crack tip are given also by equations (4.53) and (4.54), where the stress intensity factors are:*

* It should be emphasized that these results are only valid for small λ and that for large λ one must consider more terms of the asymptotic expansions. Using the method described previously on the alternate method of solution, the stress intensity factors have been determined numerically for $\nu = \frac{1}{3}$ and $\sigma^{(b)} = 0$ and may well be approximated within a 6% error and for all λ by the simple relations:

$$k_1^{(e)} = \sqrt{c} (1 + 0.317 \lambda^2)^{\frac{1}{2}}$$

and

$$k_1^{(e)} = \sqrt{c} (1 + 0.05 \lambda^2)^{\frac{1}{2}} .$$

(i) for an axial crack (see Figure 6)

$$k_1^{(e)} = \bar{\sigma}^{(e)} \sqrt{c} \left\{ 1 + \frac{5\pi\lambda^2}{64} \right\} + \bar{\sigma}^{(b)} \frac{(1-v^2)^{\frac{1}{2}} \lambda^2 \sqrt{c}}{\sqrt{3(3+v)}} \left\{ \frac{5+37v}{96(1-v)} + \frac{1+5v}{16(1-v)} \cdot \left(\gamma + \ln \frac{\lambda}{8} \right) \right\} + O(\lambda^4 \ln \lambda); \quad \lambda < 1 \quad (4.70a)$$

$$k_1^{(b)} = -\bar{\sigma}^{(e)} \sqrt{c} \frac{\sqrt{3} \lambda^2}{(1-v^2)^{\frac{1}{2}}} \left\{ \frac{5+37v}{96} + \frac{1+5v}{16} \left(\lambda + \ln \frac{\lambda}{8} \right) \right\} - \bar{\sigma}^{(b)} \sqrt{c} \left\{ 1 - \frac{1+2v+5v^2}{(3+v)(1-v)} \frac{\pi\lambda^2}{64} \right\} + O(\lambda^4 \ln \lambda); \quad \lambda < 1 \quad (4.70b)$$

(ii) for a peripheral crack (see Figure 4.7)

$$k_1^{(e)} = \bar{\sigma}^{(e)} \sqrt{c} \left\{ 1 + \frac{\pi\lambda^2}{64} \right\} + \bar{\sigma}^{(b)} \frac{(1+v^2)^{\frac{1}{2}} \lambda^2 \sqrt{c}}{\sqrt{3(3+v)}} \left\{ \frac{(1+v)}{32(1-v)} + \frac{(1+v)}{16(1-v)} \left(\lambda + \ln \frac{\lambda}{8} \right) \right\} + O(\lambda^4 \ln \lambda); \quad \lambda < 2.5 \quad (4.71a)$$

$$k_1^{(b)} = -\bar{\sigma}^{(e)} \frac{\sqrt{3} \lambda^2 \sqrt{c}}{(1-v^2)^{\frac{1}{2}}} \left\{ \frac{1+v}{32} + \frac{1+v}{16} \left(\gamma + \ln \frac{\lambda}{8} \right) \right\} - \frac{\bar{\sigma}^{(b)}}{3+v} \left\{ 1 - \frac{5+2v+v^2}{(3+v)(1-v)} \frac{\pi\lambda^2}{64} \right\} + O(\lambda^4 \ln \lambda); \quad \lambda < 2.5 \quad (4.71b)$$

(iii) for an arbitrary orientation crack* (see Figure 4.8)

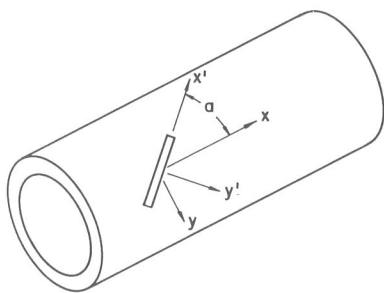


Figure 4.8

$$k_1^{(e)} = \bar{\sigma}^{(e)} \sqrt{c} \left\{ 1 + \frac{(5 \cos^2 \alpha + \sin^2 \alpha) \pi \lambda^2}{64} \right\} + \bar{\sigma}^{(b)} \frac{(1-v^2)^{\frac{1}{2}} \lambda^2 \sqrt{c}}{\sqrt{3(3+v)}}$$

$$\left\{ \left[\frac{5+37\nu}{96(1-\nu)} + \frac{1+5\nu}{16(1-\nu)} \left(\gamma + \ln \frac{\lambda \cos \alpha}{8} \right) \right] \cos^2 \alpha + \left[\frac{1+\nu}{32(1-\nu)} + \frac{1+\nu}{16(1-\nu)} \left(\gamma + \ln \frac{\lambda \sin \alpha}{8} \right) \right] \sin^2 \alpha \right\} + O(\lambda^4 \ln \lambda); \quad \lambda < 1 \quad (4.72a)$$

$$k_1^{(b)} = -\bar{\sigma}^{(e)} \frac{\sqrt{3} \lambda^2 \sqrt{c}}{(1-\nu^2)^{\frac{3}{2}}} \left\{ \left[\frac{5+37\nu}{96} + \frac{1+5\nu}{16} \left(\gamma + \ln \frac{\lambda \cos \alpha}{8} \right) \right] \cos^2 \alpha + \left[\frac{1+\nu}{32} + \frac{1+\nu}{16} \left(\gamma + \ln \frac{\lambda \sin \alpha}{8} \right) \right] \sin^2 \alpha \right\} - \bar{\sigma}^{(b)} \sqrt{c} \left\{ 1 - \frac{(1+2\nu+5\nu^2) \cos^2 \alpha + (5+2\nu+\nu^2) \sin^2 \alpha}{(3+\nu)(1-\nu)} \frac{\pi \lambda^2}{64} \right\} + O(\lambda^4 \ln \lambda); \quad \lambda < 1 \quad (4.72b)$$

and*

$$k_2^{(e)} = \bar{\tau}^{(e)} \sqrt{c} \left\{ 1 + \sqrt{5} \frac{\pi \lambda^2}{64} \sin 2\alpha \right\} + \bar{\tau}^{(b)} \sqrt{c} \frac{(1-\nu^2)^{\frac{1}{2}} \lambda^2}{\sqrt{3(3+\nu)}} \left[\frac{5+37\nu}{96(1-\nu)} + \frac{1+5\nu}{16(1-\nu)} \left(\gamma + \ln \frac{\lambda \cos \alpha}{8} \right) \right]^{\frac{1}{2}} \left[\frac{(1+\nu)}{32(1-\nu)} + \frac{(1+\nu)}{16(1-\nu)} \left(\gamma + \ln \frac{\lambda \sin \alpha}{8} \right) \right]^{\frac{1}{2}} \sin 2\alpha + O(\lambda^4 \ln \lambda); \quad \lambda < 1 \quad (4.73a)$$

$$k_2^{(b)} = \bar{\tau}^{(e)} \frac{\sqrt{3} \lambda^2 \sqrt{c}}{(1-\nu^2)^{\frac{3}{2}}} \left\{ \left[\frac{5+37\nu}{96} + \frac{1+5\nu}{16} \left(\gamma + \ln \frac{\lambda \cos \alpha}{8} \right) \right]^{\frac{1}{2}} \left[\frac{1+\nu}{32} + \frac{1+\nu}{16} \left(\gamma + \ln \frac{\lambda \sin \alpha}{8} \right) \right]^{\frac{1}{2}} \sin 2\alpha + \bar{\tau}^{(b)} \sqrt{c} \left\{ 1 + \frac{(5\nu_0^2 - 12\nu_0 + 8)^{\frac{1}{2}} (\nu^2 + 2\nu + 5)^{\frac{1}{2}}}{(4-\nu_0)\nu_0} \frac{\pi \lambda^2}{64} \sin 2\alpha \right\} \right\} + O(\lambda^4 \ln \lambda); \quad \lambda < 1 \quad (4.73b)$$

4.6 Approximate stress intensity factors for other shell geometries

Because the complementary or perturbed solution presents contributions only in the immediate vicinity of the crack tip, one may consider—at least

* The reader should note that the angular distribution here is given by equations (4.61) and (4.62).

locally – the principal radii or curvatures constant. Thus, assuming that the crack is parallel to one of the principal axes, say along the x -axis, one may hypothesize that the stress intensity factors depend primarily on the curvatures that one observes as he travels along and perpendicular to the crack prolongation. Consequently, one may estimate the stress intensity factors by a proper superposition of the results of an axial and a peripheral crack in a cylindrical shell. In particular, for $\bar{\sigma}^{(b)} = 0$

$$k_1^{(e)} \simeq \bar{\sigma}^{(e)} \sqrt{c} \left\{ 1 + \frac{\pi \lambda_x^2}{64} + \frac{5\pi \lambda_y^2}{64} \right\} + O(\lambda^4 \ln \lambda); \quad \lambda < 1 \quad (4.74a)$$

$$k_1^{(b)} \simeq \bar{\sigma}^{(e)} \frac{\sqrt{3} \sqrt{c}}{(1 - \nu^2)^{\frac{1}{2}}} \left\{ \frac{5 + 37\nu}{96} \lambda_x^2 + \frac{1 + 5\nu}{16} \lambda_y^2 \left(\gamma + \ln \frac{\lambda_y}{8} \right) \right. \\ \left. + \frac{1 + \nu}{32} \lambda_x^2 + \frac{1 + \nu}{16} \lambda_x^2 \left(\gamma + \ln \frac{\lambda_x}{8} \right) \right\} + O(\lambda^4 \ln \lambda); \quad \lambda < 1 \quad (4.74b)$$

In order to check the validity of such a superposition we will consider as our first example* a spherical cap the stress intensity factors for which we know exactly.

Example 1: Sphere. For this shell the curvature is constant in all directions; therefore, in view of equations (4.70a) and (4.71a), one has

$$k_1^{(e)} \simeq \bar{\sigma}^{(e)} \sqrt{c} \left\{ 1 + \frac{\pi \lambda^2}{64} + \frac{5\pi \lambda^2}{64} \right\} = \bar{\sigma}^{(e)} \left\{ 1 + \frac{3\pi \lambda^2}{32} \right\}; \quad \lambda < 1 \quad (4.75)$$

which is identical to equation (4.56). Similarly,

$$k_1^{(b)} \simeq -\bar{\sigma}^{(e)} \frac{\sqrt{3} \lambda^2 \sqrt{c}}{(1 - \nu^2)^{\frac{1}{2}}} \left\{ \frac{5 + 37\nu}{96} + \frac{1 + 5\nu}{96} \left(\gamma + \ln \frac{\lambda}{8} \right) \right. \\ \left. + \frac{1 + \nu}{32} + \frac{1 + \nu}{16} \left(\gamma + \ln \frac{\lambda}{8} \right) \right\} \\ = -\bar{\sigma}^{(e)} \frac{\sqrt{3} \lambda^2 \sqrt{c}}{(1 - \nu^2)^{\frac{1}{2}}} \left\{ \frac{-0.1 + 5\nu}{32} + \frac{1 + 3\nu}{8} \left(\gamma + \ln \frac{\lambda}{4} \right) \right\}; \quad \lambda < 1 \quad (4.76)$$

which agrees fairly well with equation (4.57). One may conclude, therefore, that such a hypothesis may not be unreasonable.

* In the following examples, we have assumed $\sigma^{(b)} = 0$.

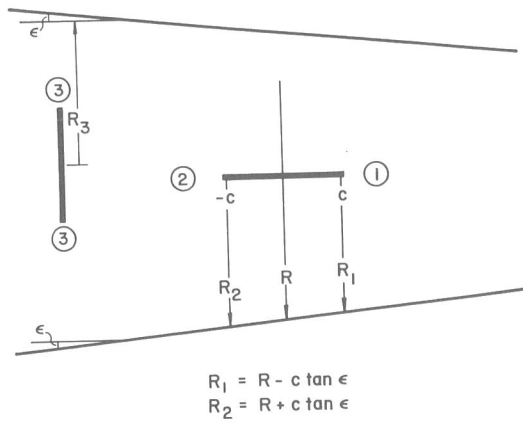


Figure 4.9. Conical Circular Shell

Example 2: Circular conical shell (see Figure 4.9). In this case, one curvature is infinite, the other finite; therefore,

(i) for an axial crack:

$$k_1^{(e)} \simeq \bar{\sigma}^{(e)} \sqrt{c} \left\{ 1 + \frac{5\pi}{64} \lambda_1^2 \right\}; \quad \lambda_1 < 1 \quad (4.77a)$$

$$k_1^{(e)} \simeq \bar{\sigma}^{(e)} \sqrt{c} \left\{ 1 + \frac{5\pi}{64} \lambda_2^2 \right\}; \quad \lambda_2 < 1 \quad (4.77b)$$

(ii) for a peripheral crack:

$$k_1^{(e)} \simeq \bar{\sigma}^{(e)} \sqrt{c} \left\{ 1 + \frac{\pi}{64} \lambda_3^2 \right\}; \quad \lambda_3 < 1 \quad (4.78)$$

where

$$\lambda_1^2 \equiv [12(1 - \nu^2)]^{\frac{1}{2}} \frac{c^2}{(R - c \tan \epsilon)h}$$

$$\lambda_2^2 \equiv [12(1 - \nu^2)]^{\frac{1}{2}} \frac{c^2}{(R + c \tan \epsilon)h}$$

$$\lambda_3^2 \equiv [12(1 - \nu^2)]^{\frac{1}{2}} \frac{c^2}{R_3 h} \quad (4.79)$$

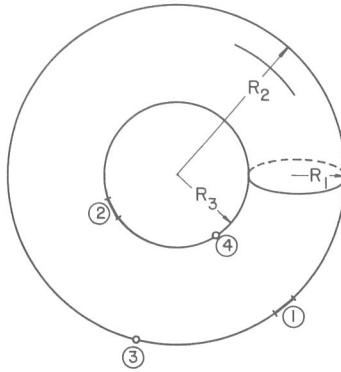


Figure 4.10. Toroidal Shell

Example 3: Toroidal shell (see Figure 4.10). For an axial crack in the outer surface

$$k_1^{(e)} \simeq \bar{\sigma}^{(e)} \sqrt{c} \left\{ 1 + \frac{5\pi}{64} \lambda_1^2 + \frac{\pi}{64} \lambda_2^2 \right\}; \quad \lambda_{1,2} < 1 \quad (4.80)$$

for an axial crack in the inner surface

$$k_1^{(e)} \simeq \bar{\sigma}^{(e)} \sqrt{c} \left\{ 1 + \frac{5\pi}{64} \lambda_1^2 - \frac{\pi}{64} \lambda_3^2 \right\}; \quad \lambda_{1,3} < 1 \quad (4.81)$$

for a peripheral crack in the outer surface

$$k_1^{(e)} \simeq \bar{\sigma}^{(e)} \sqrt{c} \left\{ 1 + \frac{5\pi}{64} \lambda_2^2 + \frac{\pi}{64} \lambda_1^2 \right\}; \quad \lambda_{1,2} < 1 \quad (4.82)$$

and for a peripheral crack in the inner surface

$$k_1^{(e)} \simeq \bar{\sigma}^{(e)} \sqrt{c} \left\{ 1 - \frac{5\pi}{64} \lambda_3^2 + \frac{\pi}{64} \lambda_1^2 \right\}; \quad \lambda_{1,3} < 1 \quad (4.83)$$

4.7 Plates on elastic foundations

Analyses of plates resting on foundations usually fall into two groups. The first group follows the well known theory of Winkler and Zimmerman [23] in which the elastic foundation is considered as a system of separate unconnected springs. Such a hypothesis simplifies considerably the analysis of

structures on elastic foundations and leads frequently to incorrect results. The second group follows the theory in which one describes the physical properties of the natural foundation more accurately by the hypothesis that the foundation is an elastic isotropic semi-infinite space [24]. Here again, such a hypothesis leads to cumbersome calculations and therefore the method becomes impractical.

Recently a new theory based on Vlasov's general variational method [25] has been proposed [26]. This theory considers the elastic foundation as a single or double layer model whose properties are described by two or more generalized elastic characteristics. The advantage of this theory is that it is more accurate than the theory of Winkler and Zimmermann and simpler than the theory of the elastic semi-infinite space.

Winkler-Zimmermann Foundation. The characteristics of the fracture of plates resting on a Winkler-Zimmermann foundation have been investigated and the results are reported in references [27] and [28]. In this case, the governing differential equation for the displacement function $w(x, y)$, with x and y as dimensionless coordinates (see Figure 4.11), is given in the classical theory by

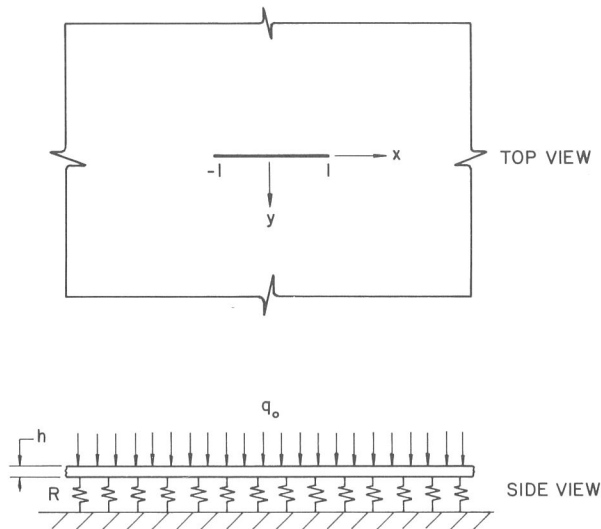


Figure 4.11

$$(\nabla^4 + \lambda^4) w(x, y) = \frac{q(x, y)c^4}{D}, \quad (4.84)$$

where

$$\lambda^4 \equiv \frac{k}{D} c^4 \quad (4.85)$$

and k the elastic foundation spring constant. In reference [27], the author, using the method described in section 4.3, was able to obtain an asymptotic expansion of the solution for small values of the parameter λ . Thus without going into the details, the stresses at the surface $z = h/2c$ are given by equations (4.54) where the bending stress intensity factor now is given by

$$k_1^{(b)} = \bar{\sigma}^{(b)} \sqrt{c} \left\{ 1 + \frac{3 + 2\nu + 3\nu^2}{(3 + \nu)(1 - \nu)} \frac{\pi\lambda^2}{32} + \left[\frac{3 + 6\nu + 15\nu^2}{(3 + \nu)(1 - \nu)} \left(\gamma + \ln \frac{\lambda}{4} \right) + \frac{3\nu^2 - 1}{(3 + \nu)(1 - \nu)} \right] \frac{\lambda^4}{128} \right\}^{-1} + O(\lambda^6 \ln \lambda); \quad \lambda < 2 \quad (4.86)$$

On the other hand, for large values of the parameter λ reference [28] gives

$$k_1^{(b)} = \bar{\sigma}^{(b)} \sqrt{c} \frac{1}{\sqrt{\lambda}} + O(\lambda^{-3/2}); \quad \lambda > 4 \quad (4.87)$$

For example, along the crack prolongation and for $\nu = 1/3$,

$$\frac{\sigma_y^{(b)}(\varepsilon, 0)}{\bar{\sigma}^{(b)}} \simeq \begin{cases} \frac{\sqrt{c}}{(2r)^{\frac{3}{2}}} \frac{1}{\left[1 + \frac{9}{5} \frac{\pi}{32} \lambda^2 \right]}; & \lambda < 1 \\ \frac{\sqrt{c}}{(2r)^{\frac{3}{2}}} \frac{1}{\sqrt{\lambda}} & ; \lambda > 4 \end{cases} \quad (4.88)$$

Since the behavior of the stress intensity factor at the two extremes is known, one may construct a curve with the proper asymptotes. Such a plot is given in Figure 4.12. One concludes, therefore, that the general effect of an elastic foundation is to decrease the stresses in magnitude by a factor which depends on the type of foundation, the crack length, and the material properties.

Single Layer Foundation. Following [26], the differential equation governing

the displacement function is $w(X, Y)$ of a plate resting on single layered elastic foundation (see Figure 4.13).

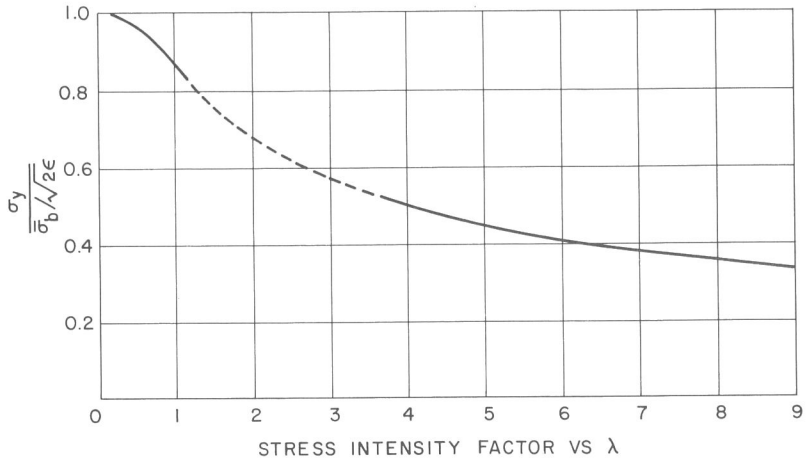


Figure 4.12

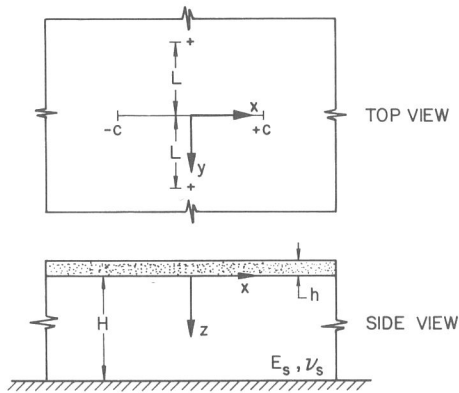


Figure 4.13. A Cracked Plate on a Single Layered Foundation

$$\nabla^4 w - 2r^{*2} \nabla^2 w + \delta^{*4} w + m^* \frac{\partial^2 w}{\partial t^2} = \frac{q}{D} \tag{4.89}$$

with the quantities r^* , δ^* and m^* as constants defined by*

$$\begin{aligned} r^{*2} &= \frac{E_s^*}{(1 + \nu_s^*)D} \int_0^H \psi^2(z) dz \\ \delta^{*4} &= \frac{E_s^*}{(1 - \nu_s^{*2})D} \int_0^H \{\psi'(z)\}^2 dz \\ m^* &= \left(\frac{\gamma_p h}{g} + \frac{\gamma_s}{g} \int_0^H \psi^2(z) dz \right) \frac{1}{D} \end{aligned} \quad (4.90)$$

and

$$\begin{aligned} E_s^* &= \frac{E_s}{1 - \nu_s^2} \\ \nu_s^* &= \frac{\nu_s}{1 - \nu_s} \end{aligned} \quad (4.91)$$

D the flexural rigidity of the plate, γ_p and γ_s the specific weights of the plate and elastic foundation and g the gravitational acceleration.

The problem of a finite crack, of length $2c$, in the plate has been investigated and the results are reported in reference [29]. Thus without going through the details, the stress intensity factor, in view of the definitions

$$r = cr^*, \quad \delta = c\delta^*, \quad k = r/\delta, \quad (4.92)$$

become

(i) for $\delta < r < 1$

$$\begin{aligned} k_1^{(b)} &= \bar{\sigma}_b \sqrt{c} (12 - \frac{3}{2}r^2) \left\{ 12 + \left\{ -\frac{3}{4}[v(2-v)(5-12\gamma+12\ln 2) + \right. \right. \\ &\quad \left. \left. - 2(3-4\gamma+4\ln 2) + 16v(1-2\gamma+2\ln 2)] + \right. \right. \\ &\quad \left. \left. + \frac{3}{2}(3v+1)(1-v)(1-\ln 2+2\ln r) \right\} \frac{r^2}{(1-v)(3+v)} + \right. \\ &\quad \left. + \left\{ \frac{3}{64}[v(2-v)(5-12\gamma+12\ln 2)(3-4\gamma+4\ln 2) - 8v(1-2\gamma+2\ln 2)] \right\} \right. \end{aligned}$$

* It is assumed that no horizontal displacements occur in the elastic foundation and that the vertical displacement is given by a single function $\psi(z)$. From reference [26] a typical function is

$$\psi(z) = \frac{\sinh [r_*(H-z)]}{\sinh [r_*H]}$$

where r_* is a coefficient determining the variation with depth of the displacement.

$$-\frac{3}{3^2}(3\nu+1)(1-\nu)\left(\frac{3}{2}-\ln 2+2\ln r\right)\left\{\frac{r^4}{(1-\nu)(3+\nu)}+\dots\right\}^{-1} \quad (4.93)$$

Notice that δ does not appear in equation (4.93) for it is negligible. A plot of this is given in Figure 4.14.

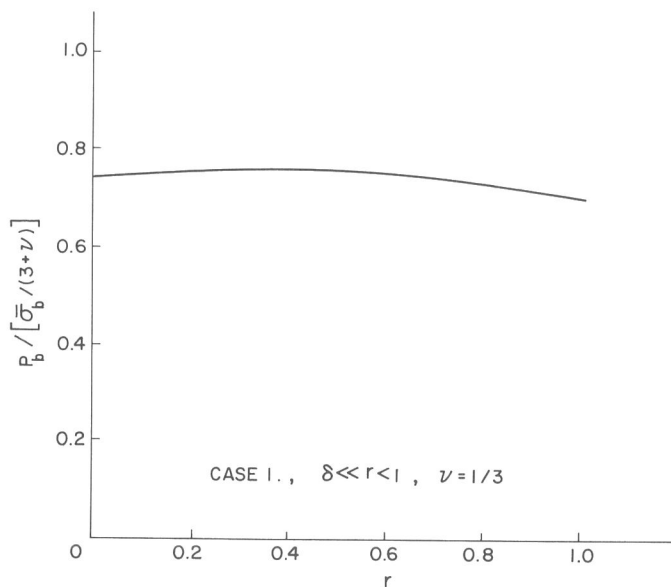


Figure 4.14. Stress Coefficient Versus r

(ii) for $r = k\delta < 1$, where k is a real constant

$$k_1^{(b)} = \bar{\sigma}_b \sqrt{c} \left\{ 1 + \frac{1}{8(k^4 - 1)^{\frac{1}{2}}} \ln \left[\frac{k^2 + (k^4 - 1)^{\frac{1}{2}}}{k^2 - (k^4 - 1)^{\frac{1}{2}}} \right] \right. \\ \left. \frac{(1 + \nu) + \frac{1}{4}(3\nu + 1)(1 - \nu)(2k^4 - 1)}{(1 - \nu)(3 + \nu)} \delta^2 \right. \\ - \frac{1}{16(1 - \nu)(3 + \nu)} [v(2 - \nu)(5 - 12\gamma + 12 \ln 2) + (3 - 4\gamma + 4 \ln 2) + \\ - 8v(1 - 2\gamma + 2 \ln 2) - 2(1 + 3v)(1 - \nu)(1 - 2 \ln 2)] k^2 \delta^2 + \\ \left. + \frac{1}{4} k^2 (\ln \delta) \delta^2 + \frac{3k^2 \delta^2}{4 - 3k^2 \delta^2} - \frac{3}{32(1 - \nu)(3 + \nu)} [v(2 - \nu) \right.$$

$$\begin{aligned}
 & (5 - 12\gamma + 12 \ln 2) + (3 - 4\gamma + 4 \ln 2) - 8\nu(1 - 2\gamma + 2 \ln 2) - 2(1 + 3\nu) \\
 & \left(\frac{1}{2} - 2 \ln 2\right) \left[\frac{k^4 \delta^4}{4 - 3k^2 \delta^2} + \frac{3}{16(k^4 - 1)^{\frac{1}{2}}} \ln \frac{k^2 + (k^4 - 1)^{\frac{1}{2}}}{k^2 - (k^4 - 1)^{\frac{1}{2}}} \right. \\
 & \left. \frac{(1 + \nu) + \frac{1}{4}(3\nu + 1)(1 - \nu)(2k^4 - 1)}{(1 + \nu)(3 + \nu)} \frac{k^2 \delta^4}{4 - 3k^2 \delta^2} + \frac{3k^4 \delta^4}{32 - 24k^2 \delta^2} \right. \\
 & \left. \ln \delta + \dots \right]^{-1} \tag{4.94}
 \end{aligned}$$

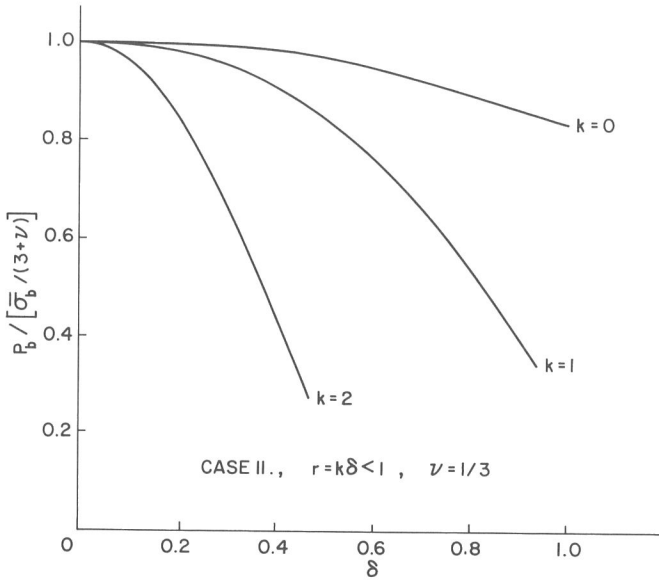


Figure 4.15. Stress Coefficient Versus δ

A plot is given in Figure 4.15. Furthermore, in the limit as $k \rightarrow 0$ one recovers the results for a Winkler and Zimmermann foundation.

4.8 Particular solutions

In general, the actual stress fields will depend upon the contributions of the particular solutions reflecting the magnitude and distribution of the applied load. On the other hand, the singular part of the solution, that is the terms producing infinite elastic stresses at the crack tip, will depend upon the local

stresses existing along the locus of the crack before it is cut, which of course are precisely the stresses which must be removed by the particular solutions described above in order to obtain the stress-free edges as required physically.

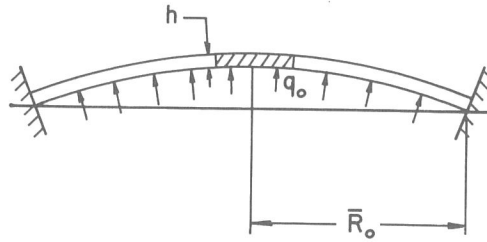


Figure 4.16. Pressurized Spherical Cap With Fixed Ends

Clamped Spherical Shell. Consider a clamped segment of a shallow spherical shell of base radius \bar{R}_0 and containing at the apex a finite radial crack of length $2c$ (see Figure 4.16). The shell is subjected to a uniform internal pressure q_0 with radial extension $N_r = (q_0/2)R$, and because it is clamped we require that the displacement and slope vanish at $\bar{R} = \bar{R}_0$. For this problem the residual 'applied bending' and 'applied stretching' loads at the crack are:*

$$\bar{\sigma}^{(e)} = q_0 R / 2h, \quad \bar{\sigma}^{(b)} = 0 \quad \text{and} \quad \bar{\tau}^{(e)} = 0 \quad (4.95)$$

Closed Cylindrical Tank. Consider a shallow cylindrical shell containing a crack of length $2c$. The shell is subjected to a uniform internal pressure q_0 with an axial extension $N_x = (q_0 R / 2)$, $M_y = 0$, far away from crack. For this problem, if the crack is parallel to the axis of the cylinder, then

$$\bar{\sigma}^{(e)} = (q_0 R / h), \quad \bar{\sigma}^{(b)} = 0 \quad \text{and} \quad \bar{\tau}^{(e)} = 0 \quad (4.96)$$

If the crack is perpendicular to the axis of the cylinder, then

$$\bar{\sigma}^{(e)} = q_0 R / 2h, \quad \bar{\sigma}^{(b)} = 0 \quad \text{and} \quad \bar{\tau}^{(e)} = 0 \quad (4.97)$$

In the event that the crack makes an angle α with the axis of the cylinder, then

* For more details see reference [30].

$$\bar{\sigma}^{(e)} = (q_0 R/4h)(3 + \cos 2\alpha), \bar{\sigma}^{(b)} = 0, \text{ and } \bar{\tau}^{(e)} = (q_0 R/4h) \sin 2\alpha \quad (4.98)$$

Infinite Plate. Consider an infinite thin plate containing a crack of length $2c$. At infinity the plate is subjected to a uniform extensional load σ_∞ and in-plane shear load τ_∞ , then

$$\bar{\sigma}^{(e)} = \sigma_\infty, \quad \bar{\sigma}^{(b)} = 0 \text{ and } \bar{\tau}^{(e)} = \tau_\infty. \quad (4.99)$$

Rectangular Strip on a Spring Foundation. Consider a rectangular strip, infinitely long in the x -direction and of finite width b in the y -direction. Furthermore, let the strip be subjected to a constant moment M_0 and zero shear at $y = \pm b$, and simultaneously subject to a uniform normal loading q_0 . Then*

$$\bar{\sigma}^{(e)} = \bar{\tau}^{(e)} = 0$$

and

$$\bar{\sigma}^{(b)} = -\frac{6M_0}{h^2 c^2} \frac{\cos(\lambda b/\sqrt{2}) \sinh(\lambda b/\sqrt{2}) + \sin(\lambda b/\sqrt{2}) \cosh(\lambda b/\sqrt{2})}{\cosh(\lambda b/\sqrt{2}) \sinh(\lambda b/\sqrt{2}) + \sin(\lambda b/\sqrt{2}) \cos(\lambda b/\sqrt{2})} \quad (4.100)$$

where

$$\lambda^4 \equiv \frac{k}{D} c^4 \quad (4.101)$$

Plate on a Single Layered Foundation. Consider an infinite elastic plate which rests on a single-layered elastic foundation and contains a finite, through the thickness, crack of length $2c$. The plate is subjected to two equal concentrated lateral static loads of intensity P_0 with corresponding points of application $(0, L, -h)$ and $(0, -L, -h)$ (see Figure 4.13). Furthermore, it will be assumed that $L \gg c$. Then**

$$\begin{aligned} \bar{\sigma}^{(e)} = 0 \text{ and } \bar{\sigma}^{(b)} = & -\frac{6D}{h^2 c^2} \frac{P_0 c^4}{2\pi D(\lambda_+^2 - \lambda_-^2)} \left\{ \frac{(1-\nu)}{(x^2 + l^2)^{\frac{3}{2}}} \left[1 - \frac{2x^2}{x^2 + l^2} \right] \right. \\ & \{ (\lambda_+ K_1 [\lambda_+ (x^2 + l^2)^{\frac{3}{2}}] - \lambda_- K_1 [\lambda_- (x^2 + l^2)^{\frac{3}{2}}]) + \\ & \left. + \frac{l^2 + \nu x^2}{x^2 + l^2} \{ \lambda_+^2 K_0 [\lambda_+ (x^2 + l^2)^{\frac{3}{2}}] - \lambda_-^2 K_0 [\lambda_- (x^2 + l^2)^{\frac{3}{2}}] \} \right\} \quad (4.102) \end{aligned}$$

* For more details see reference [28].

** See reference [29].

where

$$l = \frac{L}{c}, \quad \lambda_{\pm}^2 = r^2 \pm (r^4 - \delta^4)^{\frac{1}{2}} \quad (4.103)$$

Now, since we have already assumed that $1 \ll l$, it is easy to see that the above bending moment (along the crack) is approximately a constant, i.e., $-Dm_0/c^2$. Alternately, as an engineering approximation, one may think of the quantity $(-Dm_0/c^2)$ as an upper bound, or lower bound, or even a mean value of the precise bending moment along the crack in order to obtain an estimate of the stresses in the vicinity of the crack.

4.9 Discussion

From the above analysis it becomes evident that in an initially curved sheet the stresses near the crack tip possess the usual $1/\sqrt{r}$ singular behavior which is characteristic to two-dimensional linear elastic crack problems. Furthermore, the angular distribution around the crack tip is precisely the same as that of a flat plate and that the initial curvature appears only in the stress intensity factors and it appears in such a way that in the limit as $R \rightarrow \infty$ one recovers the flat sheet behavior.

A typical term is of the form

$$\frac{\sigma_{\text{sheet}}}{\sigma_{\text{plate}}} \simeq 1 + \left\{ \frac{a_1}{R_1} + \frac{a_2}{R_2} + \frac{b_1}{R_1} \ln \frac{c}{(R_1 h)^{\frac{1}{2}}} + \frac{b_2}{R_2} \ln \frac{c}{(R_2 h)^{\frac{1}{2}}} \right\} \cdot \frac{c^2}{h} + O\left(\frac{1}{R_1^2}, \frac{1}{R_2^2}\right) \quad (4.104)$$

Thus the general effect of a positive (negative) initial curvature, in reference to that of a flat sheet, is to increase (decrease) the stresses in the neighborhood of the crack point and reduce (increase) its resistance to fracture initiation. For a cylindrical shell with an axial crack, for example, equation (4.178) reads

$$\frac{\sigma_{\text{hoop}}}{\sigma_{\text{plate}}} \simeq \frac{1}{(1 + 0.317\lambda^2)^{\frac{1}{2}}}, \quad (4.105)$$

which correlates flat sheet behavior with that of initially curved specimens.

In a similar manner, the general effect of an elastic foundation is to decrease the magnitude of the stress intensity factor in the neighborhood of

the crack tip and as a result prevent further fracture. This decrease clearly depends on the values of the parameters which characterize the elastic foundation.

References

- [1] Ogibalov, P. M., *Dynamics and strength of shells*, translated from Russian, published for NASA and NSF by the Israel Program for Scientific Translations.
- [2] Marguerre, K., Zur theorie der gekrummten platte grosser formänderung, *Proc. 5th Int. Congr. Appl. Mech.* pp. 93–101 (1938).
- [3] Reissner, E., On some problems in shell theory, *Structural Mechanics, Proceedings of the First Symposium on Naval Structural Mechanics*, pp. 11–14, pp. 74–113 (1958).
- [4] Reissner, E., A note on membrane and bending stresses in spherical shells, *Soc. Industr. Appl. Math.* 4, pp. 230–240 (1956).
- [5] Sechler, E. E. and Williams, M. L., The critical crack length in pressurized monocoque cylinders, Final Report, GALCIT 96, Calif. Inst. Tech., September 1959. See also: M. L. Williams, *Proc. Crack Propagation Symp.*, Cranfield, 1, pp. 130 (1961).
- [6] Erdelyi, A et al., Tables of integral transforms, *Bateman Manuscript Project*, McGraw-Hill, N. Y. (1954).
- [7] Ang, D. D. and Williams, M. L., Combined stresses in an orthotropic plate having a finite crack, *J. Appl. Mech.*, pp. 372–378 (1961).
- [8] Noble, B., The approximate solution of dual integral equations by Variational Methods, *Proceedings Edinburgh Mathematical Society*, 11, pp. 113–126 (1958–59).
- [9] Muskhelishvili, N. I., *Singular integral equations*, English translation by J. R. M. Radok, P. Noordhoff, Ltd., The Netherlands (1953).
- [10] Folias, E. S., *The stresses in a spherical shell containing a crack*, ARL 64–23, Aerospace Research Laboratories (1964).
- [11] Folias, E. S., *The effect of initial curvature on cracked flat sheets*, UTEC DO 68–070, University of Utah (1968).
- [12] Sneddon, I. N. and Lowengrub, M., *Crack problems in the classical theory of elasticity*, John Wiley & Sons, Inc., New York (1969).
- [13] Kantorovich, L. V. and Krylov, V. I., *Approximate methods of higher analysis*, P. Noordhoff, The Netherlands (1964).
- [14] Folias, E. S., On the predictions of catastrophic failures in pressurized vessels, *Perspectives of Fracture Mechanics*, edited by G. C. Sih, H. C. van Elst and D. Broek, Noordhoff International Publishing (1974).
- [15] Williams, M. L., The bending stress distribution at the base of a stationary crack, *J. Appl. Mech.*, pp. 78–82 (1961).
- [16] Knowles, J. K. and Wang, N. M., On the bending of an elastic plate containing a crack, *J. Math. and Phys.* 39, pp. 223–236 (1960).
- [17] Sih, G. C. and Hagendorf, H. C., A new theory of spherical shells with cracks, *Thin Shell Structures*, edited by Y. C. Fung and E. E. Sechler, Prentice-Hall, pp. 519–545 (1974).

- [18] Williams, M. L., On the stress distribution at the base of a stationary crack, *J. Appl. Mech.* (1957).
- [19] Do, S. H. and Folias, E. S., On the steady-state transverse vibrations of a cracked spherical shell, *International Journal of Fracture Mechanics*, 7, No. 1, pp. 23-37 (1971).
- [20] Folias, E. S., On the steady-state transverse vibrations of a cracked plate, *Engineering Fracture Mechanics Journal*, Vol. 1, No. 2, pp. 363-368 (1968).
- [21] Folias, E. S., An axial crack in a pressurized cylindrical shell, *International Journal of Fracture Mechanics*, 1, 2, pp. 104-113 (1965), or The stresses in a cylindrical shell containing an axial crack, ARL-64-174, Aerospace Research Laboratories, United States Air Force, Dayton, Ohio, pp. 1-42 (1964).
- [22] Folias, E. C., A circumferential crack in a pressurized cylindrical shell, *International Journal of Fracture Mechanics*, 3, 1, pp. 1-11 (1967).
- [23] Zimmermann, H., *Die berechnung des eisenbahn oberbaues*, Berlin: W. Ernst U. Sohn (1888).
- [24] Boussinesq, J., *Application des potentiels à l'étude de l'équilibre et du mouvement des solides élastiques*, Paris: Gauthier-Villars (1888).
- [25] Vlasov, V. Z., *General theory of shells and its application in engineering*, Moskva Leningrad, Gostekhizdat (1949).
- [26] Vlasov, V. Z. and Leont'ev, U. N., *Beams, plates and shells on elastic foundations*, NASA Technical Translation No. TTF-357 (Acc. No. TT65-50135).
- [27] Folias, E. S., On a plate supported by an elastic foundation and containing a finite crack, *International Journal of Fracture Mechanics*, 6, 3 pp. 257-263 (1970).
- [28] Ang, D. D., Folias, E. S. and Williams, M. L., The bending stress in a cracked plate on an elastic foundation, *J. Appl. Mech.*, 30, pp. 245-251 (1963).
- [29] Lin, Si-Tsai, and Folias, E. S., On the fracture of highway pavement, *International Journal of Fracture*, 11, pp. 93-106 (1975).
- [30] Folias, E. S., A finite line crack in a pressurized spherical shell, *International Journal of Fracture Mechanics*, 1, 1, pp. 20-46 (1966).